



Developing Geopolymer Composites with Structural Damage Control Potential: Utilization of Blast Furnace Slag, Calcined Clay, and MWCNT

Ahmet Filazi¹ · Rüstem Yilmazel² · Muharrem Pul³

Received: 21 March 2024 / Accepted: 31 May 2024
© The Author(s), under exclusive licence to Shiraz University 2024

Abstract

An experimental investigation was carried out to develop geopolymer composites with the potential to self-control structural damage. In this study, blast furnace slag, calcined clay and multi-walled carbon nanotubes (MWCNTs) were substituted into the geopolymer matrix. Firstly, reference samples with 5%, 10% and 15% calcined clay substitution were formed in the experiments. It was observed that geopolymer composites with 10% calcined clay substitution gave the best results. Secondly, MWCNTs were substituted at 0.25%, 0.5%, 1.0% and 1.5% to geopolymer concrete samples with 10% calcined clay substitution. The effect of increasing MWCNT amount on the electrical properties of geopolymer concrete was investigated. SEM/EDS, XRD analyses, microstructure and phase investigations were also carried out. 1% MWCNT substitution added to the sample prepared with 10% calcined clay substitution was found to give the best result compared to other addition ratios. This experimental study is very important for the design of durable and long-lasting structures in the field of structural engineering. The study is also necessary for structural damage control of geopolymer composites. This study aimed to make new geopolymer composite structures more durable and to provide good electrical conductivity. Thus, it shows that it can shed light on further research.

Keywords Geopolymer · BFS · Clay · MWCNT · Phase analysis · Microstructure · Mechanical properties · Electrical properties

1 Introduction

Geopolymers are inorganic materials resulting from the alkali activation of aluminosilicates. Aluminosilicate source materials can occur naturally, such as kaolin, metakaolin, rice husk ash, and volcanic rock dust. Additionally, they can be produced as a result of industrial processes such as metakaolin, fly ash and blast furnace slag (Nawaz et al. 2020; Khalid and Shobha 2023). Geopolymers are among the fastest-growing groups of polymeric materials. Therefore,

interest in these inorganic ceramic materials is constantly increasing. Geopolymers are used as a replacement for Portland cement in the construction industry due to their properties such as acid resistance, low porosity, low drying shrinkage, and high strength. Geopolymers are cheaper to produce than Portland cement. It also results in lower carbon dioxide emissions (Drabczyk et al. 2023). Geopolymer concrete has aimed to reduce the environmental impact of the construction materials industry. For this reason, it has attracted great interest as an alternative to OPC-based materials (Dieu and Castel 2023). Ordinary portland cement (OPC) production is responsible for approximately 1.35 billion tonnes of carbon dioxide per year. It also accounts for 5–8 per cent of greenhouse gas emissions worldwide. It is expected to reduce the dependence on OPC for concrete construction. In addition, it can also significantly benefit the environment by reducing carbon dioxide emissions. As a result, geopolymer concrete has emerged as a potential alternative to traditional cement concrete (Kamal et al. 2023). Nanomaterials used in construction can reduce global warming and significantly

✉ Ahmet Filazi
ahmetfilazi@kku.edu.tr

¹ Department of Construction, Kırıkkale Vocational School, Kırıkkale University, Kırıkkale, Turkey
² Department of Electronics and Automation, Kırıkkale Vocational School, Kırıkkale University, Kırıkkale, Turkey
³ Department of Electrical and Energy, Kırıkkale Vocational School, Kırıkkale University, Kırıkkale, Turkey

reduce costs by improving the properties of traditional materials. For this reason, they can offer a sustainable alternative to traditional materials such as cement and fly ash (Akbar et al. 2021). In the study carried out by Aygörmez, it was supported that geopolymers are sustainable and promising products according to the results of experiments with waste granite powder and fly ash (Yurdakul 2022).

Geopolymers are also composite structures. The sectors where composite materials are most widely used are the construction industry. These geopolymer composites are formed by combining various materials together. Among these materials, carbon-based nanomaterials are becoming increasingly common. The recent rapid development of nanotechnology has led to significant advances in building materials for the construction industry. In particular, there is intense research activity focused on carbon nanotubes (CNTs) (Hawreen et al. 2019), carbon nanofibers (Xingyi et al. 2018), nano carbon black (Heydar and Yilmaz 2021) and other nano-structured materials (Arabacı Egemen and Bekir Yılmaz Pekmezci 2021). In this context, carbon nanotubes (CNTs) stand out as an important reinforcement for different purposes in building materials, especially in cementitious products (Younesi et al. 2015, 2012). Among the most attractive properties of CNTs are their superior mechanical, physical, electrical, and surface area characteristics (Chong and Garboczi 2002). CNTs have high stiffness and axial strength because they have carbon-carbon sp² bonds composed of graphitic layers. Therefore, they can act as a bridge preventing crack formation in cement-based materials (Morsy et al. 2011; T. N. M. Nguyen Tri et al. 2020). Carbon nanotubes are divided into two main groups: single-walled (SWCNT) and multi-walled (MWCNT) (Ismael Mustafa 2022).

These developments have paved the way for innovative material options in the construction sector. Some of the studies identified in the literature review on the subject are summarized in Table 1.

This study investigates whether geopolymer composites have the potential for self-monitoring structural damage. The study examines the substitution of high furnace slag, calcined clay, and multi-walled carbon nanotubes (MWCNTs) in the geopolymer matrix. The experiments were conducted in two stages: In the first stage, reference samples with 5%, 10%, and 15% calcined clay substitutions were prepared. In the second stage, geopolymer concrete samples with 10% calcined clay substitution were substituted with 0.25%, 0.5%, 1.0%, and 1.5% MWCNTs.

The experiments revealed that geopolymer composites with 10% calcined clay substitution provided the best results. It was also found that samples with 10% calcined clay and 1% MWCNT substitution gave the best results compared to other substitution ratios. The study emphasizes that a suitable mixture of blast furnace slag,

calcined clay, and MWCNTs can make the structures more durable and electrically monitorable.

In this study, new generation nanomaterial substituted geopolymer composites were developed and their strength properties and electrical conductivity were investigated. Geopolymer composite structures were obtained by using blast furnace slag (BFS), calcined clay and MWCNTs at different ratios. Tests and analyses were carried out to determine the mechanical and physical properties of the new material. Furthermore, this study aims to provide potential future material options for more durable and long-lasting structures in the fields of structural engineering and materials science. As a result, this research was conducted to contribute to the development of geopolymer composites and to increase their potential for use.

2 Materials and Methods

2.1 Materials

2.1.1 Multi-Walled Carbon Nanotube (MWCNT)

Multi-walled carbon nanotubes (MWCNTs) have been preferred to improve the mechanical performance of cement-based materials since they have mechanical properties such as tensile strength ranging from 60 to 190 GPa and Young's modulus of 1.0 TPa (Moraes et al. 2015; MacKenzie and Bolton 2009). In this study, multi-walled carbon nanotubes (MWCNTs) with 92% purity, 8–10 nm outer and 5–8 nm inner diameter, 1–3 micron length and 240 m²/g specific surface area were used as additives from Nanografi Nanoteknoloji Turkey (Company of the Nanografi 2019). SEM images of the MWCNT at different magnifications and EDS analysis are given in Fig. 1 and Table 2.

2.1.2 Calcined Clay

Calcined clay is a type of clay that changes its shape by firing at high temperatures (usually between 800 °C and 1000 °C). Its structure and chemical properties change with the removal of water content and organic matter. This material is used in the production of cement, ceramics, refractory products and additives. It is known for its ability to provide high strength, thermal durability and chemical resistance. Chemically, it usually contains aluminum oxide (Al₂O₃) and silicon dioxide (SiO₂). SEM images and EDS graph of the calcined clay at different magnifications are given in Fig. 2. EDS analysis values are also given in Table 3.

Table 1 Some studies in the literature using different methods and materials

Reference	Material	Examined features
(Sawarkar et al. 2023)	High-calcium fly ash	Compressive strength, flexural strength, elasticity, heat of hydration, shrinkage deformation
(Burciaga-Díaz et al. 2020)	Waste glass, kaolinite and metakaolin	Compressive strength, FT-IR, XRD, SEM, EDS, NMR
(Torres-Carrasco and Puertas 2015)	Waste glass, fly ash	Compressive strength, pore size distribution, XRD and FTIR, NMR, BSEM/EDX
(Zhidan et al. 2015)	Nano-SiO ₂ , ultra-fine fly ash, ultra-high performance cementitious composites	Compressive strength, flexural strength, hydration, DTA/TG, X-ray, Pore structure, SEM
(Congqi et al. 2022)	Nano-SiO ₂ , nano-CaCO ₃ , nano-TiO ₂	Compressive strength, hydration heat, TG, XRD, MIP, SEM, NMR
(Gowda et al. 2017)	Nano-alumina, Cement	Compressive strength, fire resistance, workability
(Babalu and Pimplikar 2022)	Fly ash, Nano-silica	Concrete microstructure, compressive Strength, water permeability, RCPT, Water absorption
(Vivek et al. 2021)	Fine aggregate, Cement, Coarse aggregate, Nano SiO ₂	Compressive strength, splitting tensile strength
(Hisham M. Khater and El-Nagar 2020)	Silica fumes, glass waste powder, metakaolin, blast furnace slag	FTIR, XRD, DTG, compressive strength, SEM
(H. M. Khater and Abd El Gawaad 2016)	Slag geopolymeric mortar, MWCNT	XRD, FTIR, SEM, compressive strength, water absorption and drying shrinkage
(Zijian et al. 2020)	Carbon nanotube geopolymer Composite	Mechanical properties, electrical properties, durability, microstructure
(Panjasil et al. 2018)	High calcium fly ash geopolymer composite, short carbon fiber	Mechanic properties, electrical properties, microstructure
(Buchit et al. 2021)	High calcium fly ash, MWCNT	Physical properties, mechanical properties, flow diameter, electrical resistivity, piezoelectric effect
(Meng et al. 2022)	Basalt fiber, (NaOH, KOH, Ca(OH) ₂	Mechanical property, morphology,
(Saafi et al. 2013)	Low-calcium fly ash, sodium silicate, sodium hydroxide	SEM, mechanical characterization, electrical conductivity, piezoresistive response
(Enrique et al. 2017)	CNT, cement-matrix composites	Electrical conductivity, sensitivity analyses, waviness, agglomeration
(H. K. Kim et al. 2014a, b)	Silica fume, CNT, cement composites	SEM, compressive strength and porosity, electrical resistance
(H. K. Kim et al. 2014a, b)	CNT, silica fume, cement composites	Piezoresistivity, electrical resistance
(G. M. Kim et al. 2017)	CNT, cement composites	Electrical resistivity, numerical simulations
(Hieu et al. 2020)	Textile-reinforced mortar, Carbon fiber textiles	Failure modes, shear crack propagation, cracking shear stress, ultimate shear stress, crack deformation, and residual shear stress
(Yu et al. 2014)	Ultra-High Performance Hybrid Fibre Reinforced Concrete	Static and dynamic properties
(Alireza et al. 2024)	Fiber concrete Steel fiber Polypropylene fiber	Direct shear strength compressive strengthtensile strength
(Leone et al. 2018)	Fiber reinforced concrete Recycled steel fibers	Shear behaviour

2.1.3 Blast Furnace Slag (BFS)

Granulated blast furnace slag (GBFS) is also among the materials used in the production of AAS mortars. BFS was obtained from Bolu cement factory. BFS is a waste material formed by melting iron ore in a blast furnace and usually contains components such as iron oxide, silicon dioxide and calcium oxide. The density of this material ranges from 2.0 to 3.0 g/cm³. Particle sizes can also be on the micron or

millimeter scale. GBFS can have high porosity. SEM images and EDS analysis of the BFS are given in Fig. 3. EDS analysis values are also given in Table 4.

Materials used as alkaline activators include sodium hydroxide (NaOH) and sodium silicate solution (Na₂SiO₃) in solid form with 98% purity. 26.5% SiO₂, 8.3% Na₂O and 6.2% dH₂O. The sand used in the preparation of geopolymers is standard sand according to ASTM C778 and is a material used for mortar preparation.

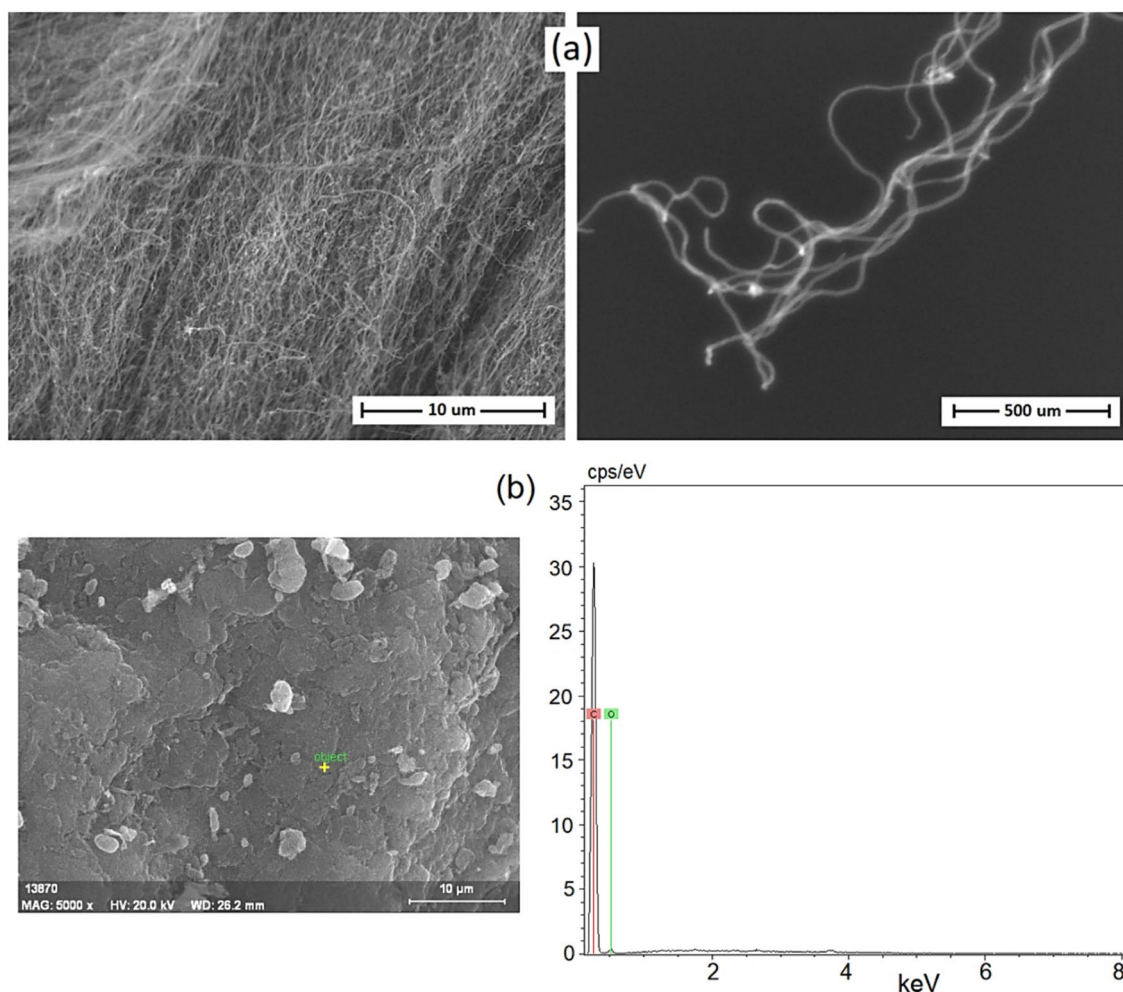


Fig. 1 MWCNT SEM a [36] image and EDS graph b

Table 2 MWCNT EDS analysis

Element	Series	Net	Unn.C (wt.-%)	Norm.C (wt.-%)
Carbon	K series	90,480	85.32	85.32
Oxygen	K series	1380	14.68	14.68

2.2 Experimental Studies

2.2.1 Production of Geopolymer Composites

When interacting with each other or with water molecules, the samples may agglomerate. The agglomerations may adversely affect the properties of the nanotubes and cause a decrease in the properties of the composite structure. Therefore, it is preferred to homogenize the nanotubes by appropriate sonication process and then use them in order to obtain a homogeneous distribution of MWCNTs in water. Dispersion was carried out with a sonicator to obtain a

homogeneous mixture by preventing agglomeration of the MWCNT reinforcement material. The stages of this process are shown in Fig. 4.

To obtain geopolymer composite materials, two stages were carried out. Firstly, S0 coded geopolymer composite without clay and MWCNT substitution was produced as a reference sample. Then, for comparison with sample S0, geopolymer composites coded S1, S2 and S3 were prepared by substituting calcined clay at different ratios. Secondly, MWCNTs were substituted at different ratios on the S2 sample (10% clay), which gave the best results. At this stage, samples S2-1, S2-2, S2-3 and S2-4 were obtained. The components are carefully mixed and standardized in specific quantities. The mixing ratios of the materials used in the composite production are shown at Table 5.

In the first phase of the study, the basic components of the geopolymer composites were selected. These components are clay, MWCNT, BFS (Blast Furnace Slag), NaOH (10 M), Na_2SiO_3 , sand and water. Then a geopolymer composite

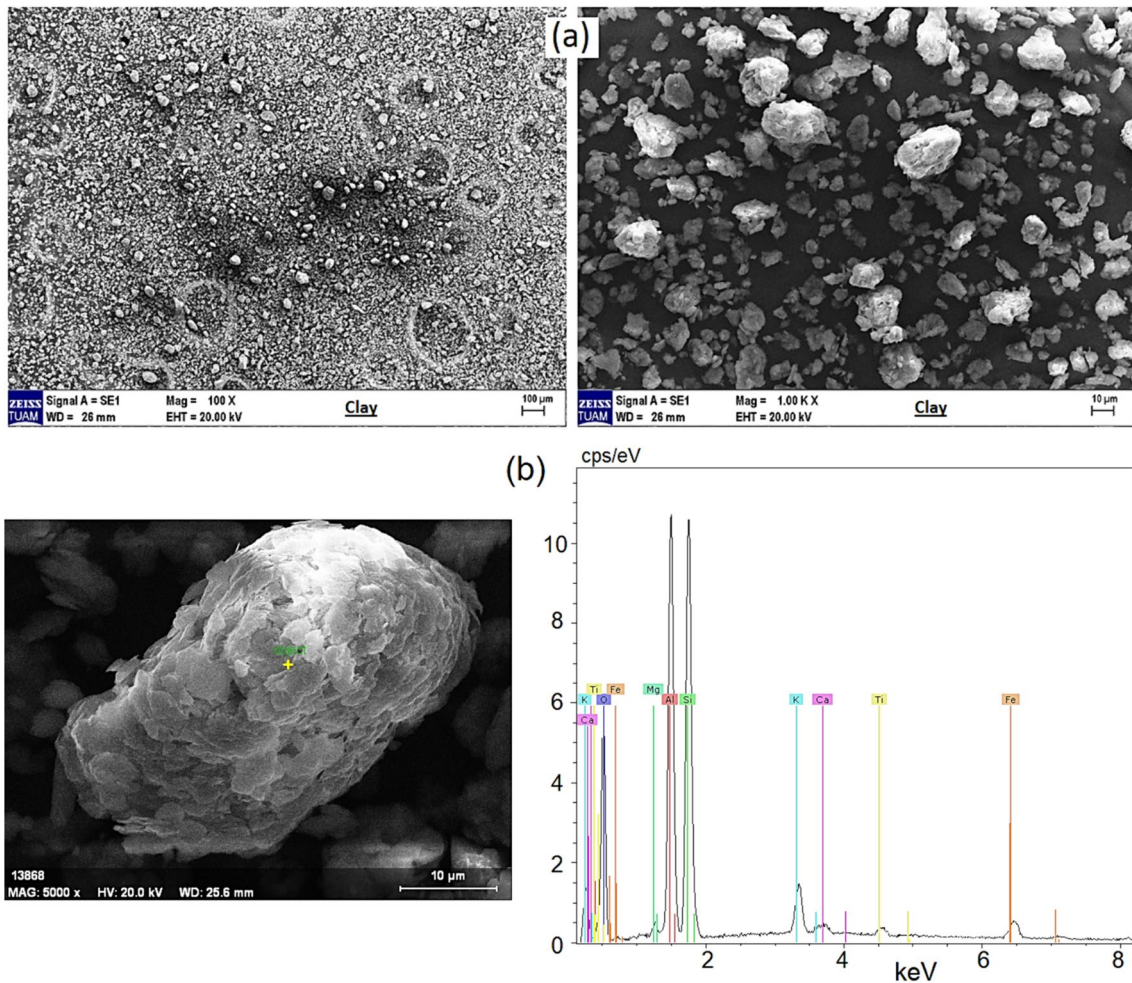


Fig. 2 Calcined clay SEM image a and EDS graph b

Table 3 Calcined clay EDS analysis

Element	Series	Net	Unn.C (wt.-%)	Norm.C (wt.-%)	Oxid	Oxid. C (wt.-%)
Magnesium	K	868	0.49	0.48	–	–
Aluminium	K	43,954	20.68	20.19	Al ₂ O ₃	38.89
Silicon	K	46,432	25.04	24.45	SiO ₂	53.32
Potassium	K	7484	2.32	2.27	K ₂ O	2.79
Calcium	K	2255	0.68	0.66	CaO	0.94
Titanium	K	1488	0.52	0.51	TiO ₂	0.87
Iron	K	3486	1.90	1.86	Fe ₂ O ₃	2.71
Oxygen	K	18,878	50.80	49.59	–	–

coded S0 without clay and MWCNT was produced. For comparison with sample S0, samples S1, S2 and S3 were produced by substituting different proportions of calcined clay. These samples represent different clay percentages. The amount of BFS, NaOH (10 M) and Na₂SiO₃ were not changed. Mechanical tests were carried out to determine the mechanical strength of the produced S0, S1, S2 and S3 samples. The highest values in flexural and compressive strength

tests were obtained from S2 sample with 10% calcined clay reinforcement.

In the second stage, MWCNT was added to the geopolymer production. MWCNTs were substituted to the 10% clay reinforced S2 specimen with the best mechanical strength at different ratios. New samples coded S2-1, S2-2, S2-3 and S2-4 were produced. In this production process, the amount of BFS, NaOH (10 M) and Na₂SiO₃

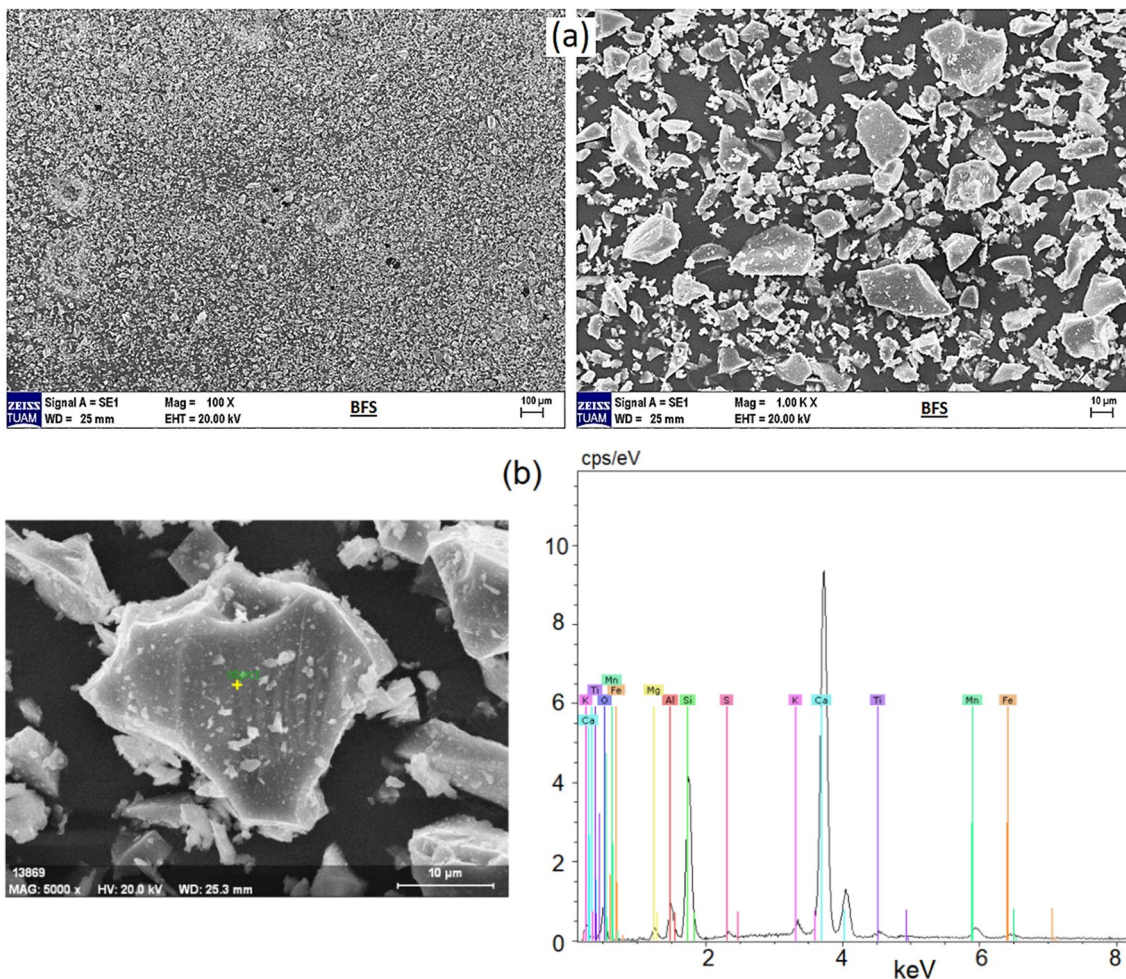


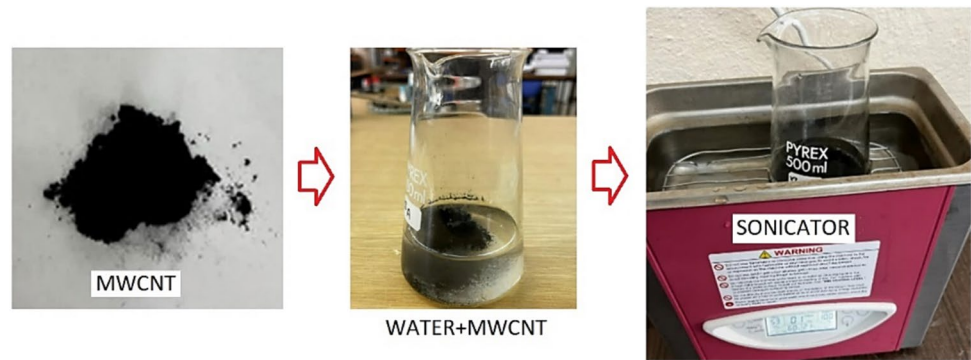
Fig. 3 Blast furnace slag (BFS) SEM image a and EDS graph b

Table 4 Blast Furnace Slag EDS analysis

Element	Series	Net	Unn.C (wt.-%)	Norm.C (wt.-%)	Oxid	Oxid. C (wt.-%)
Magnesium	K	1	0.00	0.00	—	—
Aluminium	K	2042	1.54	1.83	Al ₂ O ₃	3.61
Silicon	K	16,506	11.05	13.07	SiO ₂	29.23
Sulfur	K	1	0.00	0.00	SO ₃	0.00
Potassium	K	2101	1.20	1.42	K ₂ O	1.79
Calcium	K	56,144	34.70	41.06	CaO	60.06
Titanium	K	992	0.80	0.95	TiO ₂	1.65
Manganese	K	1950	1.88	2.22	MnO	3.00
Iron	K	351	0.37	0.44	Fe ₂ O ₃	0.65
Oxygen	K	3044	32.98	39.02	—	—

were kept constant. Production of geopolymer composites was completed by standardizing each sample to have specific amounts of BFS, NaOH (10 M), Na₂SiO₃, sand and

water. The stages of the production process are shown in Fig. 5.

Fig. 4 Dispersion of MWCNT**Table 5** Mixing ratios applied in the preparation of geopolymer composites

The first stage							
Sample code	Clay (%)	MWCNT (%)	BFS (g)	NaOH (g) (10 M)	Na ₂ SiO ₃ (g)	Sand (g)	Water (g)
S0	0	0	450	32	127	1350	146
S1	5	0	427.5	32	127	1350	146
S2	10	0	405	32	127	1350	146
S3	15	0	382.5	32	127	1350	146
The second stage							
S2-1		0.25					
S2-2	10	0.5	405	32	27	1350	146
S2-3		1					
S2-4		1.5					

2.2.2 Particle Size Analysis

In this study, a laser-assisted grain size measuring device, model number BT-9300Z, was used. This device can precisely determine grain size distributions between 0.1 μm and 1250 μm . Using the Mie Scattering Principle, the device analyzes the grain size of powdered materials in a liquid medium. Grain size distribution profiles were obtained by ensuring homogeneous distribution of the materials. The Betsize BT-9300Z model is a grain size analyzer in accordance with industry standards and offers a wide range of applications.

2.2.3 Flow Test

Workability of fresh mortar samples was evaluated according to TS EN 1015–3 standard. The tests were carried out using the methods and parameters specified in this standard. Flow value is an important parameter for determining the plasticity and flowability properties of mortars.

The TS EN 1015–3 standard is a widely used reference point for evaluating the workability of cement and mortars. The flow values were used to determine the workability properties and working processes of geopolymer

composites. These values have been an important research tool in evaluating the effects of different composite components on workability. The flow values obtained according to the TS EN 1015–3 standard are important factors in evaluating the applicability of geopolymer composites with the potential for self-control of structural damage.

2.2.4 Flexural and Compressive Strength

Compressive strength tests were conducted to assess the mechanical strength of the geopolymer composites. The geopolymer mortar mixtures were cured for 24 h under laboratory conditions at room temperature. The samples were then removed from the molds and air cured at 25 ± 3 °C. Compressive and flexural strength tests were performed on 50*50*50 mm cubes and 40*40*160 mm bars in accordance with ASTM C109 and ASTM C348, respectively. All experiments were carried out with waiting periods of 7 and 28 days.

2.2.5 Microstructural Analysis

Scanning electron microscope (SEM) was used for microstructural analysis and energy distribution spectrometer (EDS) method was used for elemental analysis.

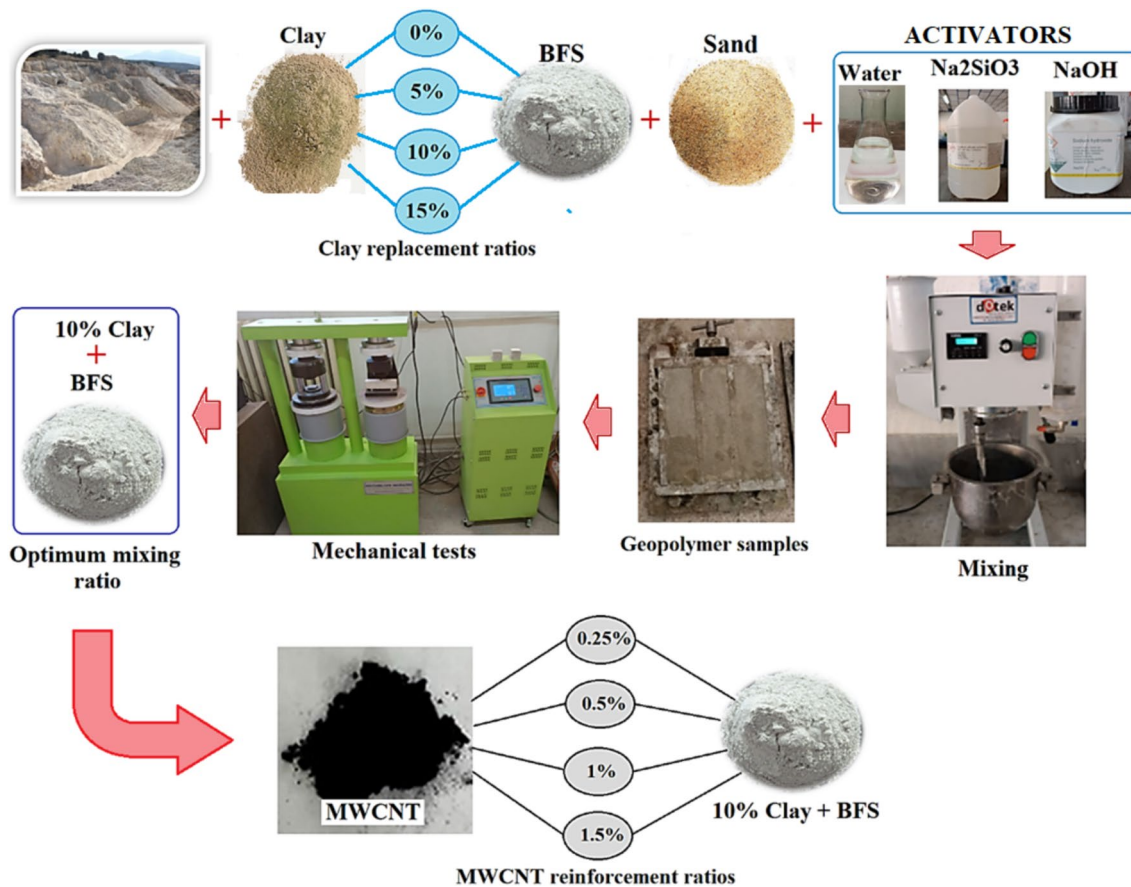


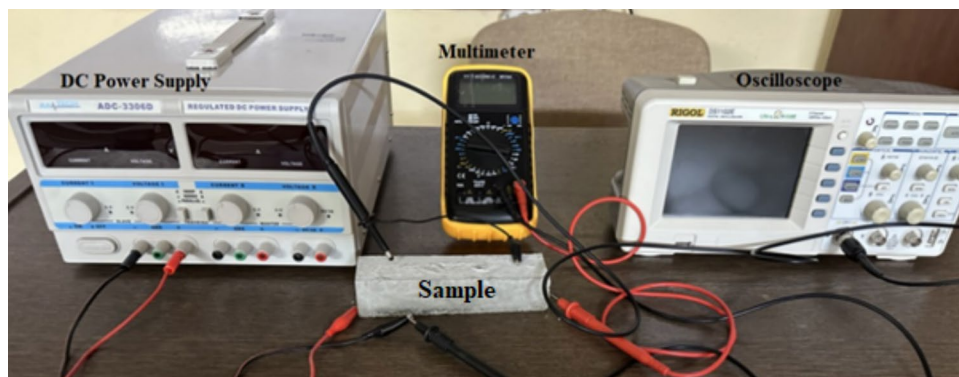
Fig. 5 Stages in the preparation of geopolymer composites

SEM imaging and EDS analysis were performed on a ZEISS LEO 1430VP scanning SEM device. Shi-madzu XRD-6000 LabX model device was used to investigate the phase structures of geopolymer composites. This device enabled phase analysis by X-Ray Diffraction (XRD) method. The surface morphology and structural details of the geopolymer composites were examined by SEM analysis. In XRD analysis, the crystalline structures of the materials and the compositions of possible phase changes were examined.

2.2.6 Measurement of Electrical Properties

Conductivity tests were performed to characterize the electrical properties. Material samples were subjected to electrical conductivity measurements using appropriate test setups. These tests were performed to evaluate the electrical conductivity behavior of the materials and to determine their electrical properties for potential applications. The electrical measurement setup is shown in Fig. 6.

Fig. 6 Two-point electrical conductivity measurement setup



In the electrical conductivity experiment, two-point direct current electrical conductivity measurement method was applied. In the experimental setup prepared for this experiment, a direct current power supply and two avometers were used. The voltage source was applied to the ends of the material. Thanks to this voltage, a voltage is created at the ends of the material. According to the sample resistance value, a current passes through it and the resistance of the composite material is determined by this electric current.

If the voltage between the ends of the material is called V and the current flowing through it is called I , the resistance (R) of the material is calculated as in Eq. 1.

$$R = \frac{V}{I} \tag{1}$$

Then, the electrical resistivity of the material is calculated using Eq. 2. Here, L represents the length of the material, A represents its cross-sectional area, and r represents its electrical resistivity.

$$r = \frac{R.A}{L} \tag{2}$$

In the last stage, after calculating the electrical resistivity of the sample, the electrical conductivity value is found by using Eq. 3.

$$s = \frac{1}{r} \tag{3}$$

3 Findings and Discussion

3.1 Particle Size Analysis

This analysis was performed to understand the dimensional properties of the additives in the geopolymer composite material.

3.1.1 Blast Furnace Slag (BFS)

The results obtained from dimensional analysis tests for Blast Furnace Slag (BFS) are shown in Fig. 7 and Table 6.

According to the BFS particle size analysis report in Fig. 7; Median Particle Size (D_{50}) is $16.68 \mu\text{m}$. This value means that 50% of the particles have diameters smaller than $16.68 \mu\text{m}$ and the other 50% have larger diameters. Volume Average Diameter ($D_{[4,3]}$) is $20.31 \mu\text{m}$. This parameter represents a volume-weighted average of the particle distribution and indicates the overall size average. Surface Average Diameter ($D_{[3,2]}$) is $4.436 \mu\text{m}$. Represents the surface-weighted average particle diameter. This value is important for applications where surface interactions are decisive. Span is 2.586. The span value indicates the width of the particle size distribution. A low span value indicates a homogeneous distribution, while a high span value indicates a wider variation in size. Specific Surface Area (SSA) is $500.9 \text{ m}^2/\text{kg}$. This value measures the surface area of particles per unit mass. A high SSA value indicates the surface reactivity and efficiency of the

Fig. 7 BFS particle size analysis

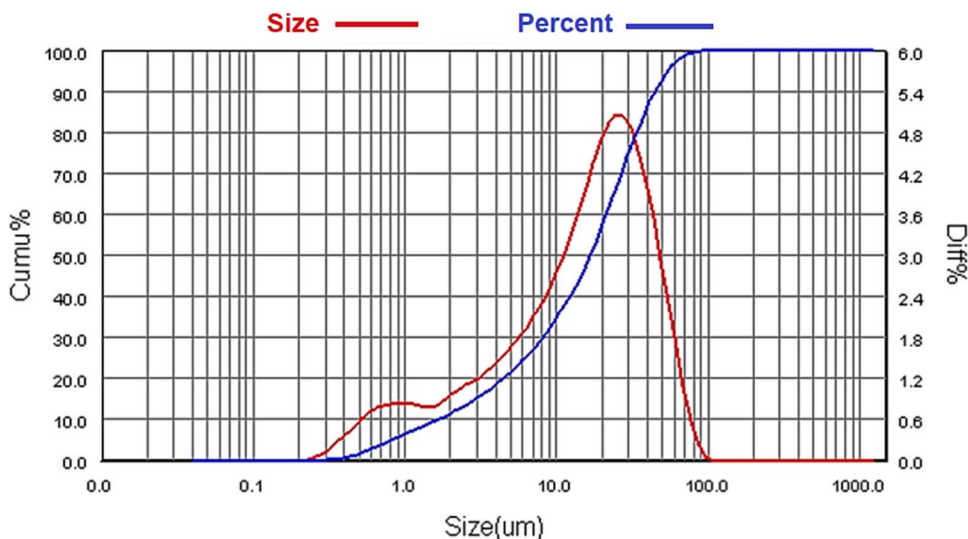
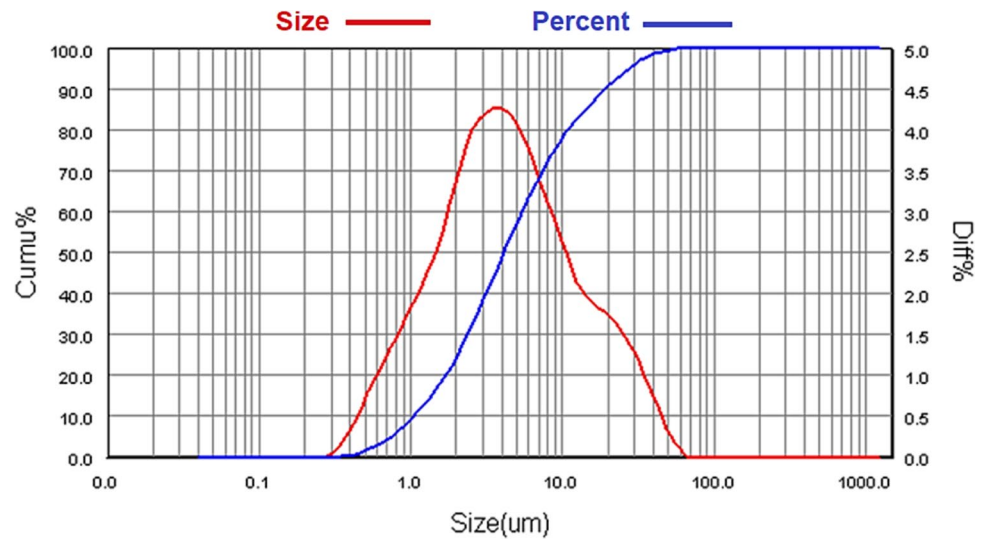


Table 6 BFS particle size analysis

Size (um)	0.5	1.0	2.0	5.0	10.0	20.0	45.0	75.0	100.0
Percent	1.68	6.38	11.41	21.59	34.66	57.09	90.13	99.23	99.98

Fig. 8 Calcined clay particle size analysis**Table 7** BFS particle size analysis

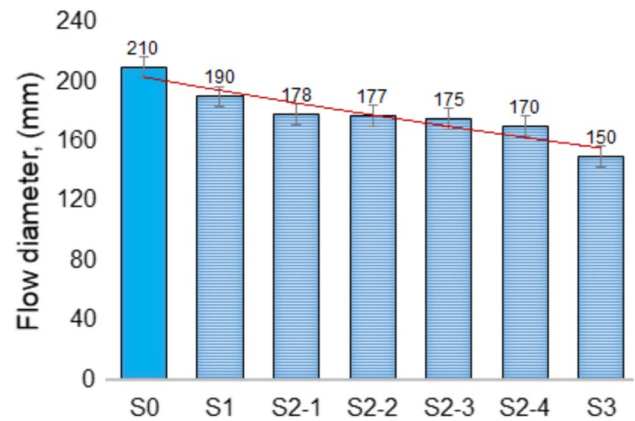
Size (µm)	0.1	0.2	0.5	1.0	2.0	5.0	10.0	20.0	45.0	75.0
Percent	0.0	0.0	1.49	9.23	24.38	57.17	77.85	90.52	99.24	100.0

material. This particle size analysis presents in detail the percentage distribution of different sized particles of blast furnace slag and important size values.

3.1.2 Calcined Clay

The results obtained from dimensional analysis tests for calcined clay are shown in Fig. 8 and Table 7.

According to the calcined clay particle size analysis report in Fig. 8; D50 (Median Particle Size) is 4.114 µm. This value means that 50% of the particles in calcined clay have diameters smaller than 4.114 µm and the other 50% have larger diameters. Volume Average Diameter (D[4,3]) is 7.465 µm. This parameter represents a volume-weighted average of the particle distribution and indicates the overall volumetric average of the particles in calcined clay. Surface Average Diameter (D[3,2]) is 2.518 µm. The surface-weighted average particle diameter indicates the average diameter of the particles represented by the surface area. This value is important for the surface reactivity and efficiency of calcined clay. Span is 4.444. The span value indicates the width of the particle size distribution. A lower span value indicates a more homogeneous distribution, while a higher span value indicates a wider variation in size. Specific Surface Area (SSA) is 882.4 m²/kg. This value measures the surface area of particles per unit mass. A high SSA value reflects the surface reactivity and efficiency of calcined clay.

**Fig. 9** Flow test results

3.1.3 Flow Test

The graph created according to the flow tests of geopolymer composite materials is given in Fig. 9. When Fig. 9 is examined, it is seen that the amount of flow in other samples decreased compared to S0 sample. S1 sample decreased by 9.53%, S2-1 sample by 15.24%, S2-2 sample by 15.71%, S2-3 sample by 16.67%, S2-4 sample by 19.05% and S3 sample by 28.57% in terms of flow diameter. These percentage decreases indicate that clay and MWCNT substitution in the samples negatively affected the workability properties of geopolymer concrete. The samples with a higher percentage of substitution showed a greater decrease in the flow diameter.

A decrease in the flow diameter indicates that the concrete mix has a more solid and dry structure, while an increase indicates a more liquid and flowable structure. Therefore, the flow diameter results are used as an important parameter in evaluating the workability properties of geopolymers. As a result, according to the flow diameter results, the S0 sample has a more workable and more easily formable structure than the other samples. The clay and MWCNT substitution processes in the other samples reduced the flow diameters.

3.1.4 Flexural Strength Test

Geopolymer composites have become a topic of increasing interest in modern structural engineering and materials science. The mechanical properties of these composites, especially compressive and flexural strength, are critical for the durability and performance of structures. Therefore, examining the impact of different substitution processes and components on the mechanical properties of geopolymer composites can shape the use of these materials in future construction projects. The graph based on the flexural strength tests of geopolymer composite materials is given in Fig. 10.

According to the 7-day and 28-day flexural strength results of S0, which is considered as the reference sample in Fig. 10, the flexural strength increased by 5.77% at the end of 7 days and 5.60% at the end of 28 days. These values indicate that sample S0 shows a slight increase in strength with the passing time. Sample S1 is a calcined clay substitute sample. Accordingly, the 7-day and 28-day flexural strength results show an increase of 4.68% and 4.55%, respectively. This indicates that calcined clay substitution slightly increased the strength of sample S1. Similarly, sample S3 was also formed with calcined clay substitution. The 7-day and 28-day strength results of sample S3 also showed an increase. These values indicate that the calcined clay substitution increased the flexural strength of the sample over time.

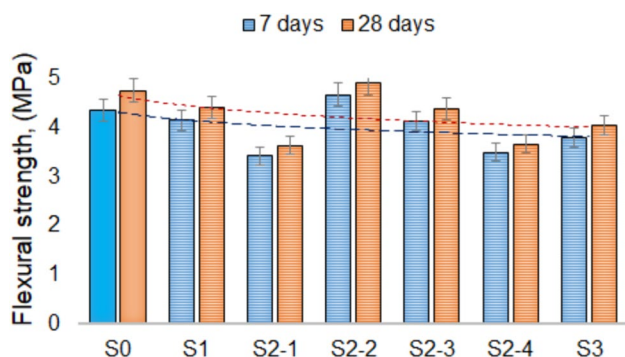


Fig. 10 Flexural strength test results

When MWCNT reinforced samples are analyzed, the effect of MWCNT substitution differs between the samples. For example, the increase in the strength of sample S2-2 after 7 days and 28 days is more apparent than the other samples. This indicates that the MWCNT substitution had a positive effect on this particular sample, while sample S2-4 shows that the MWCNT substitution caused a significant decrease in compressive strength.

In conclusion, this study provides an important contribution for structural engineers and material scientists to evaluate the performance of geopolymer composites. The effects of different substitution processes and effects on the mechanical properties of their components will form the basis for developing more durable structures in the future. This study can contribute to the further widespread of geopolymer composites in the construction industry and sustainable construction practices.

3.1.5 Compressive strength test

The data obtained from the compressive strength tests of geopolymer composite materials are given in Fig. 11.

The S0 sample was determined as the control sample of this study and was compared with other samples. These comparisons allowed us to examine the effects of the substitution treatments on the compressive strength properties in more detail. According to Fig. 11, sample S1 showed 3.2% higher strength than sample S0 at 7 days and 4.68% higher strength than sample S0 at 28 days. These values indicate that calcined clay substitution slightly increased the strength of sample S1.

Sample S2-1 shows a strength 5.1% higher than that of sample S0 at 7 days and 4.32% higher than that of sample S0 at 28 days. These results indicate that MWCNT substitution slightly increased the strength of sample S2-1. Sample S2-2 showed 15.6% higher strength than sample S0 at 7 days and 9.1% higher strength than sample S0 at 28 days. This indicates that MWCNT substitution significantly increased the strength of sample S2-2.

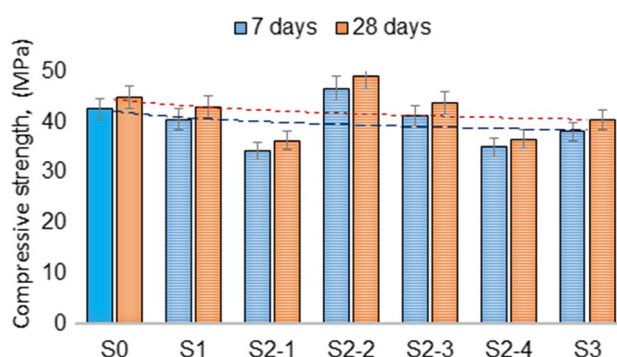


Fig. 11 Compressive strength test results

Sample S2-3 shows 2.8% higher strength at 7 days than sample S0 and 4.53% higher strength at 28 days than sample S0. These values indicate that MWCNT substitution slightly increased the strength of sample S2-3. Sample S2-4 shows a strength 15.1% higher than sample S0 at 7 days and 2.69% higher than sample S0 at 28 days. However, a significant decrease was observed in this sample. It is seen that MWCNT substitution decreases the strength of sample S2-4. Sample S3 showed a 7.5% lower strength than sample S0 at 7 days and 6.99% lower strength than sample S0 at 28 days. This result indicates that the substitution of calcined clay and MWCNT slightly reduced the strength of sample S3.

In conclusion; 7-day strength results show that substitution processes and components have significant effects on the mechanical properties of geopolymer composite samples. It was observed that MWCNT substitution caused an increase in some samples and a decrease in some samples. Calcined clay substitution also has a significant effect. According to the 28-day strength results, the performance of the samples is affected in different ways. Sample S2-2 showed a significant increase, while sample S3 showed a significant decrease. Other samples also showed strength increases or decreases at different rates. The mechanical properties of the slag geopolymer mortar were observed to increase significantly when multi-walled carbon nanotubes (MWCNTs) were added to the mixture (Abu Al-Rub Rashid et al. 2012). The addition of 0.5 wt% MWCNT increased the compressive and flexural strengths of metakaolinite-based geopolymer nanocomposites using MWCNTs at three different concentration levels (Mesgari et al. 2016). These results clearly illustrate how geopolymer composite samples are affected by different substitution processes and components.

3.1.6 Electrical Conductivity

Electrical conductivity and resistivity values of geopolymer composites containing nanocarbon reinforced blast furnace slag and clay cement are shown in Fig. 12. Electrical conductivity values obtained by adding MWCNT at different ratios to cements formed using 10% clay were compared. It

was observed that the electrical conductivity of the material increased as the amount of MWCNT added to the samples increased. At the same rate, it was observed that the electrical resistivity decreased. In particular, it is seen that the electrical conductivity of the sample formed with a 1.5% MWCNT reinforcement increases 2.25 times compared to the sample formed with 1% MWCNT. This rate corresponds to a very significant increase. This increase in electrical conductivity has more than one effect. Firstly, CNTs must interact with each other along a specific path in order to increase the electrical conductivity of the material. In other words, in order to ensure electron flow, that is, tunneling, the electrons that will provide conductivity must be less than 5 nm apart (Fangming et al. 2004). Therefore, it is natural for electrical conductivity to increase if the material produced is homogeneously distributed (Jang et al. 2023).

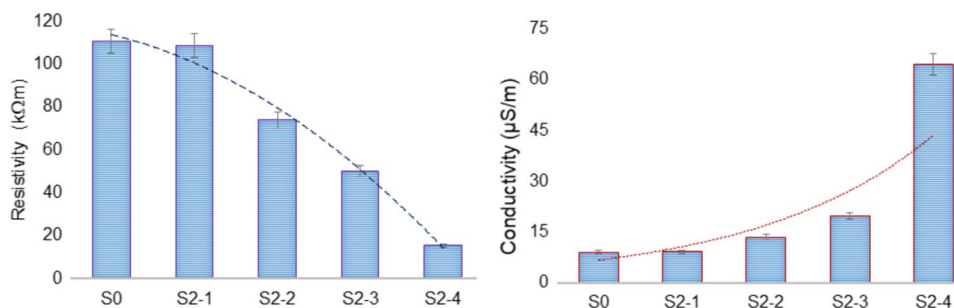
Another factor influencing electrical conductivity is the percolation threshold, which varies based on the structure and contribution rate of the materials within the sample. An increase in electrical conductivity suggests that it is either below or equal to the percolation threshold. This indicates that the added MWCNTs are evenly distributed throughout the sample. The high electrical conductivity of MWCNTs and their homogeneous distribution in the sample significantly contribute to the overall increase in electrical conductivity. These findings align with previous studies (Yoon et al. 2023; Jang et al. 2021). In Fig. 12, a decreasing trend in electrical resistivity is observed, as indicated by the dashed line. This decrease in resistivity corresponds to an increase in electrical conductivity, which is also represented by a dashed line trending upward.

3.1.7 XRD Phase Analysis

XRD (X-ray diffraction) analysis provides important information about the crystal structure and phase components of the material. The data obtained from XRD (X-ray diffraction) analysis of geopolymer composite materials are shown in Fig. 13.

The XRD data in Fig. 13 contains the diffraction intensity at a specific X-ray diffraction angle (2θ). High intensity peaks are observed at certain diffraction

Fig. 12 Resistivity and conductivity test results



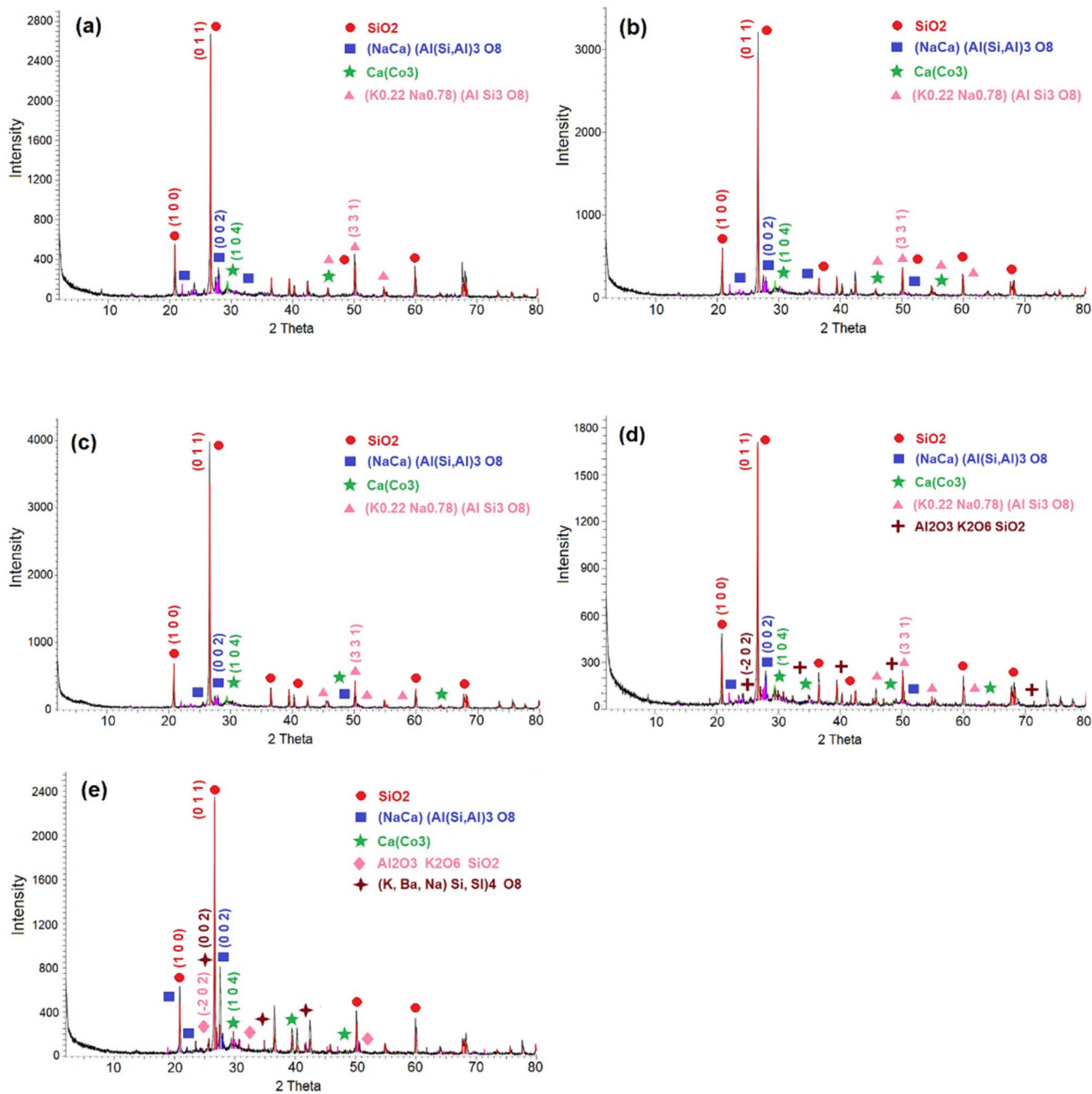


Fig. 13 XRD models of 10% Clay and a 0.25%, b 0.5%, c 1.0%, d 1.5% MWCNT, e reference sample

angles in the data set. These peaks are due to the regular arrangement of the crystal structures of the material. They also provide information about the crystal structure properties. High and sharp peaks in the graphs indicate that the crystal structure is regular and homogeneous, while low and broad peaks can be associated with structural defects or amorphous structures. Fluctuations and changes in density values indicate that the structural properties of geopolymer composites vary. It also indicates that certain crystal planes diffract more.

When 0.25% MWCNT and 10% clay reinforced geopolymer composites in Fig. 13a are examined, it is determined that SiO₂, the main phase, has a hexagonal P3121 (152) crystal structure. It is also seen that it has the most intense peak in the (0 1 1) plane at approximately 26.63-two theta degrees. This is seen to occur in the same way in all composite structures in Fig. 13b, c, d, e. It is understood that (Na, Ca) Al (Si, Al)₃ O₈ Sodium Calcium Aluminum Silicate compound, which is the other effective component in the geopolymer composite material, has the

most effective peak in the (0 0 2) plane at approximately 28.08-two theta degrees in the Triclinic C-1 (2) crystal structure. The $\text{Ca}(\text{CO}_3)$ Calcium Carbonate compound in the geopolymer is Rhombo. H.axes structure and has the most intense peak at 29.4-two theta degrees (1 0 4). The last component detected in the geopolymer composite structure in Fig. 13a is $(\text{K}_{0.22} \text{Na}_{0.78}) (\text{Al Si}_3 \text{O}_8)$ Potassium Sodium Aluminum Silicate. It is understood that the $(\text{K}_{0.22} \text{Na}_{0.78}) (\text{Al Si}_3 \text{O}_8)$ compound has the strongest peak in the (3 3 1) plane at the 51.1-two theta course on the Triclinic C-1 (2) crystal structure.

The most important reason for the highest peak of SiO_2 compound in XRD analysis is considered to be the presence of sand in the structure. Because the sand used contains 99% SiO_2 . It is understood that the calcined clay, which is 10% in the geopolymer composite, is also effective in XRD analysis. Calcined clay contains 80.1% SiO_2 and 13.6% Al_2O_3 . Therefore, SiO_2 among these two important components that make up the geopolymer composite structure formed the most intense peaks in XRD analysis.

XRD analysis of the geopolymer composite with 0.25% MWCNT and 10% clay reinforcement shows that the other important compound is $\text{Ca}(\text{CO}_3)$ Calcium Carbonate. Another one of the compounds that make up the geopolymer composite is blast furnace slag (BFS). According to the chemical structure and EDS analysis of BFS, it is seen that it contains the highest proportion of Ca element and CaO compound. Therefore, it is evaluated that the $\text{Ca}(\text{CO}_3)$ phase detected in the geopolymer composite is largely due to BF.

According to the 1.5% MWCNT reinforced geopolymer composite in Fig. 13d, it is seen that $\text{Al}_2\text{O}_3 \text{K}_2\text{O} 6\text{SiO}_2$ (Aluminum Potassium Silicate) compound is formed unlike the others. It is seen that $\text{Al}_2\text{O}_3 \text{K}_2\text{O} 6\text{SiO}_3$ has a monoclinic C_2/m (12) crystal structure and has the most intense peak in the (-2 0 2) plane at approximately 27.08-two theta degrees. The concentration of Al_2O_3 , K_2O and SiO_2 compounds in the composition of BFS and calcined clay, which are the main elements forming the geopolymer composite, is also seen in XRD analysis. The same situation is also seen in the reference sample given in Fig. 13 (e). BFS and calcined clay, which are the matrix components in the geopolymer composite structure, are clearly identified by the presence of Al_2O_3 , K_2O and SiO_2 compounds seen in the XRD analysis of the reference sample.

According to the XRD patterns given in Fig. 13, it can be observed that the amorphous components of the matrix increase with the addition of MWCNT, while the geopolymerization reaction continues. However, it is understood that the carbon-based MWCNT reinforcement materials in the geopolymer composite structures cannot be directly detected. However, the prominence and position of the crystal peaks clearly reflect the presence of the main components of the matrix and the crystal structure. The

XRD spectrum of the reference sample shows that the matrix has a more homogeneous crystal structure without the addition of MWCNT or clay. It can be stated that MWCNT and clay additions affect the crystal structure of the main matrix component BFS. It can be said that MWCNT in different weight ratios in the geopolymer can slightly affect the amorphous structure of the matrix, but the geopolymerization reaction continues in all composite structures.

A general evaluation of the XRD results reveals that MWCNT and clay additions affect the crystal structure of the BFS matrix. The addition of MWCNT was observed to cause changes in the crystalline structural components of the matrix, while the addition of clay was observed to reflect the effects on the intrinsic structure of the matrix. The results of the reference sample show in detail how the addition of MWCNT and clay changed the crystal structure of the matrix.

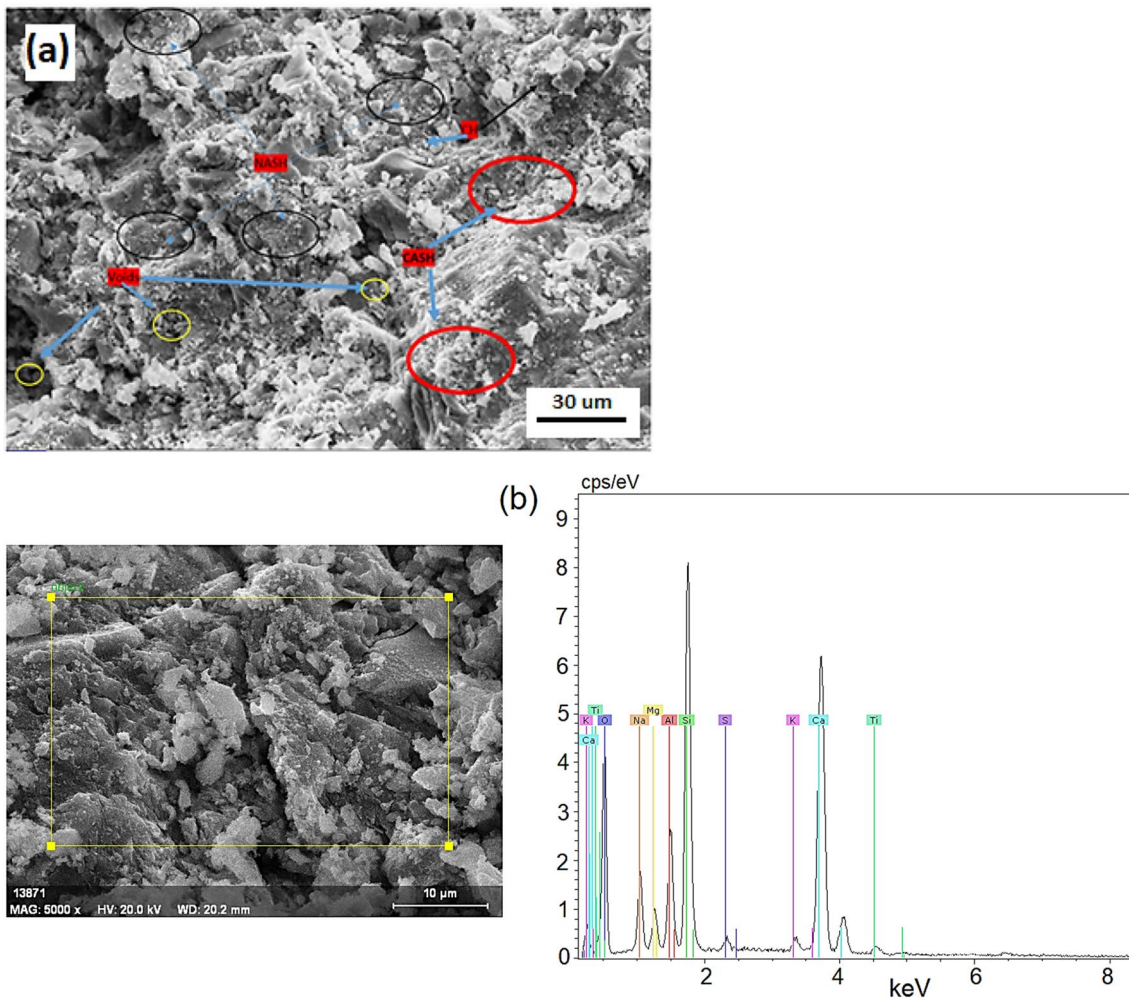
3.1.8 Microstructure and EDAX Elemental Analysis

Geopolymer concrete is a specialized building material made with geopolymeric binders instead of conventional Portland cement. When the internal structure of geopolymer concrete is analyzed, the presence of N-A-S-H (sodium aluminosilicate hydrate) or other geopolymeric binders that contribute significantly to its mechanical properties and durability is revealed. In addition, the Calcium Aluminosilicate Hydrate (C-A-S-H) component present in calcium-containing geopolymers increases durability. Si-O-Si binders, also known as silicate (Si) binders, are very important in the structure of geopolymers and define the chemical properties of the binder material (Brough and Atkinson 2002; Puertas et al. 2011; Eun et al. 2010). (Table 8)

Understanding and optimizing the internal structure of geopolymer concrete are imperative for advancing its properties. This knowledge not only influences the mechanical characteristics of the material but also holds promise for future construction applications with a focus on sustainability. To illuminate these structures, SEM (scanning electron microscopy) images were captured to examine the microstructure of geopolymer composite materials. Furthermore, EDAX analyses were conducted to identify the elements and compounds present in the geopolymer composite structures, as depicted in Figs. 14, 15, 16, 17, 18. In particular, detailed analysis of the internal structure is important for specific applications of geopolymer concretes. For instance, the optimized properties could lead to the development of structural elements for high-stress environments, seismic-prone regions, or energy-efficient buildings. Moreover, the

Table 8 S0 reference sample EDS analysis

Element	Series	Net	Unn.C (wt.-%)	Norm.C (wt.-%)	Oxid	Oxid. C (wt.-%)
Sodium	K	6001	5.48	5.23	–	–
Magnesium	K	3252	2.11	2.01	Na ₂ O	8.53
Aluminium	K	10,004	5.26	5.02	Al ₂ O ₃	11.49
Silicon	K	34,627	16.79	16.03	SiO ₂	41.49
Sulfur	K	1042	0.49	0.47	SO ₃	1.42
Potassium	K	1439	0.68	0.64	K ₂ O	0.94
Calcium	K	37,779	19.80	18.90	CaO	32.01
Titanium	K	1114	0.88	0.84	TiO ₂	1.70
Oxygen	K	15,035	53.28	50.85	–	–

**Fig. 14** SEM image (a) and EDS graph (b) of S0 reference sample

sustainability dimension can enable geopolymer concrete to be used in environmentally friendly construction projects.

According to the SEM image in Fig. 14a, important information about the internal structure of geopolymer concrete with 10% clay admixture can be obtained. These images clearly show the geopolymer matrix, which is one

of the basic building blocks of the concrete. This matrix contains geopolymeric components such as N–A–S–H (sodium aluminosilicate hydrate) or C–A–S–H (calcium aluminosilicate hydrate), which greatly contribute to the durability of geopolymer concrete.

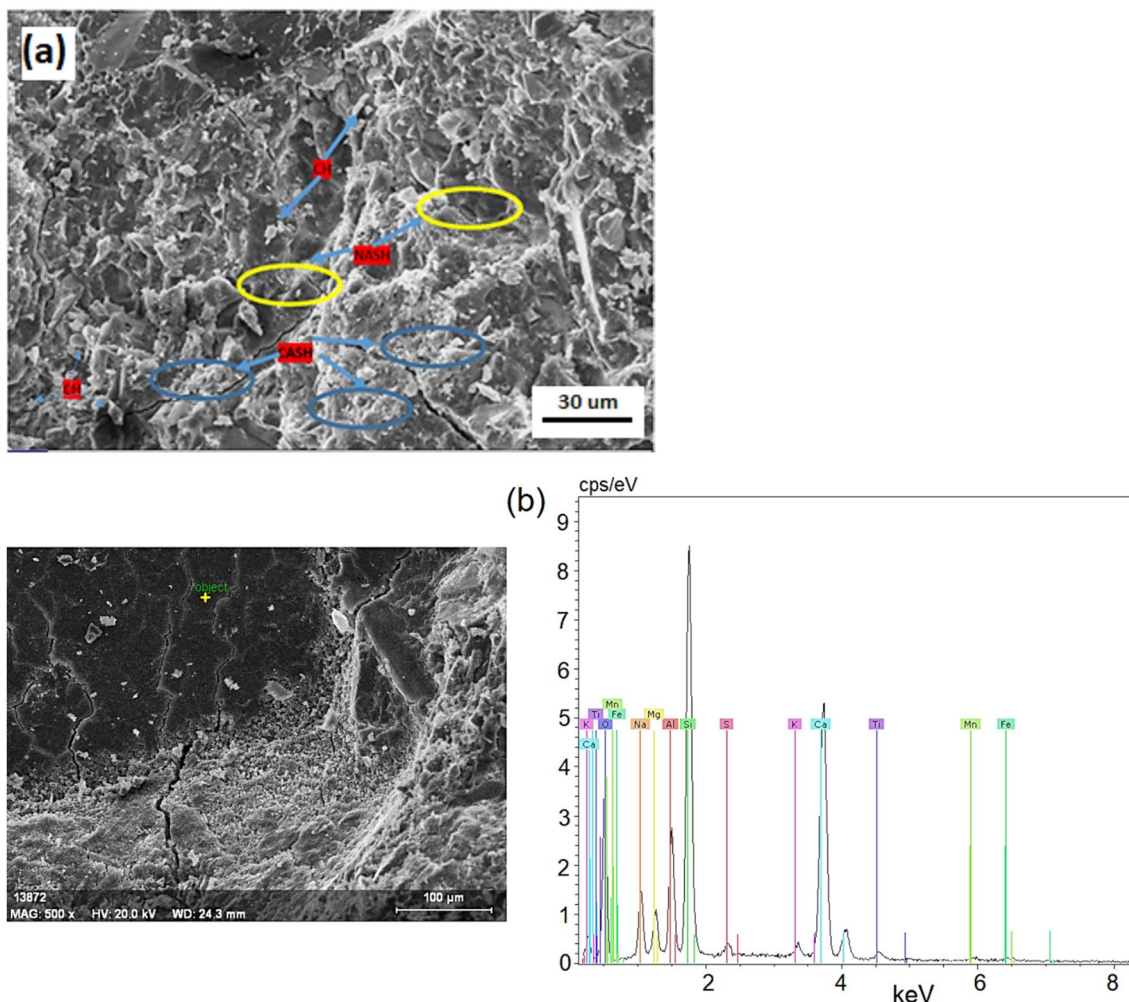


Fig. 15 SEM image **a** and EDS graph **b** of S2-1 (0.25% MWCNT + 10% Clay) geopolymer sample

According to the results of EDAX analysis, the presence of different elements such as sodium (Na), magnesium (Mg), aluminum (Al), silicon (Si), sulfur (S), potassium (K), calcium (Ca), titanium (Ti) and oxygen (O) is observed. The weight percentages of these elements determine the composition of the sample. In particular, silicon (Si) and calcium (Ca) were found in high concentrations, while other elements were found in lower concentrations. Silicon (Si) is 16.79% by weight, Aluminum (Al) 5.26% by weight and Calcium (Ca) 19.80% by weight. These ratios indicate the presence of silicate and aluminosilicate minerals. Silicon (Si) is considered the main component of silicate minerals and is present in a high proportion. Aluminum (Al) is considered a component of aluminosilicate minerals. Calcium (Ca) indicates the presence of lime or calcareous minerals.

In particular, the high concentration of silicon (Si) in SEM images indicates the presence of silica or glass-like minerals in the internal structure of the concrete. These minerals play an important role in the formation of the

geopolymer matrix and may contribute to the durability of the concrete. Furthermore, the high concentration of calcium oxide (CaO) indicates the presence of lime or calcium-containing components inside the sample. (Table 9)

According to SEM images and EDAX analysis in Fig. 15; sodium (Na), magnesium (Mg), aluminum (Al), silicon (Si), sulfur (S), potassium (K), calcium (Ca), titanium (Ti), manganese (Mn), iron (Fe) and oxygen (O) elements are present in the composite. Si is present in 17.72 wt% and Al in 5.40 wt%. These results show that silicate and aluminosilicate minerals are present in the internal structure of the sample. Silicon (Si) and aluminum (Al) are the main components of silicate and aluminosilicate minerals. SEM analysis shows that the geopolymer concrete contains geopolymeric components such as N–A–S–H (sodium aluminosilicate hydrate) or C–A–S–H (calcium aluminosilicate hydrate), which greatly contribute to the durability of geopolymer concrete. (Table 10)

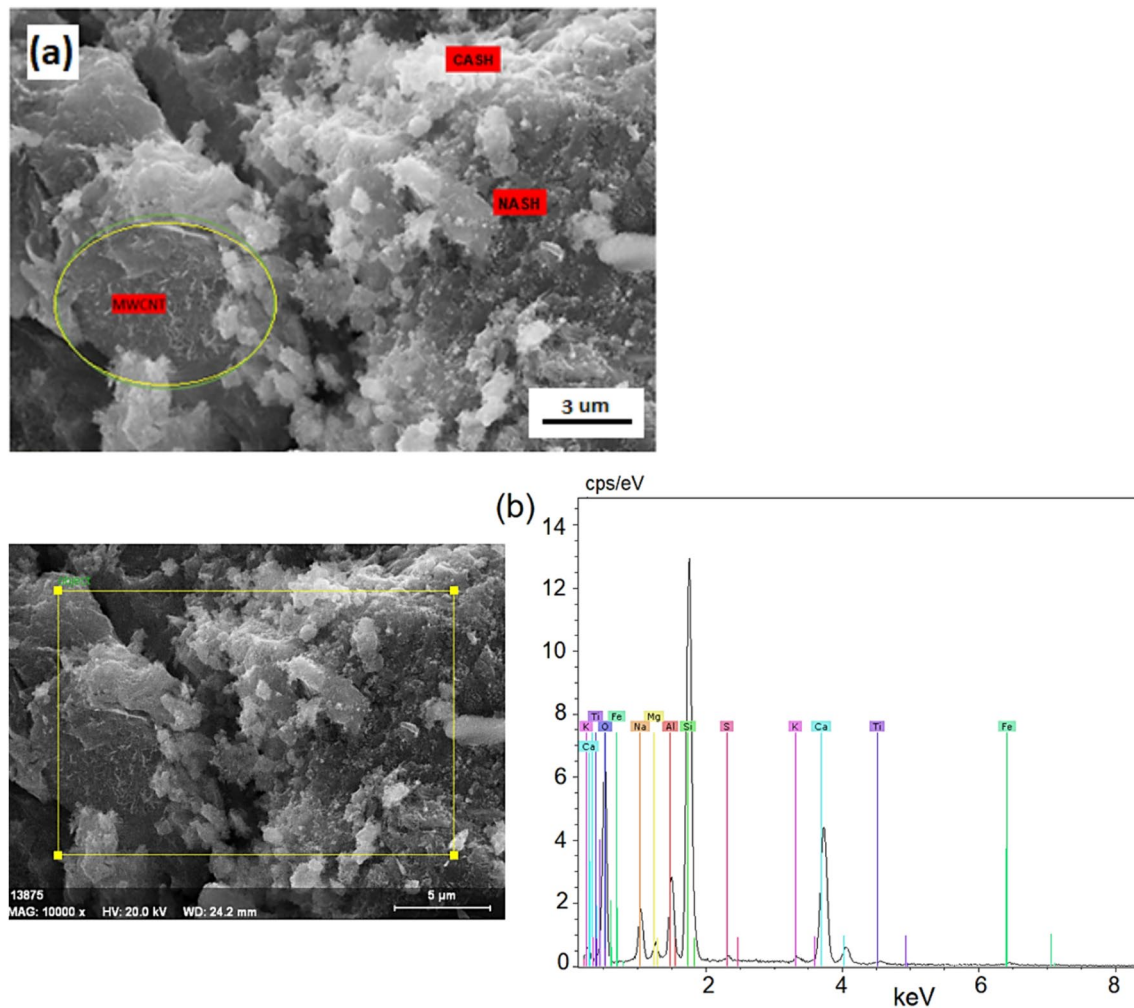


Fig. 16 SEM image **a** and EDS graph **b** of S2-2 (0.5% MWCNT + 10% Clay) geopolymer sample

It can be seen in Fig. 16 that there are various elements in the chemical composition of the 0.5% MWCNT + 10% Clay reinforced sample. The percentages of these elements are important factors determining the composition and properties of the sample. Especially silicon (Si), calcium (Ca) and oxygen (O) are present in high percentages. The SEM analysis in Fig. 16a shows that MWCNT is particularly prominently detected. This result indicates the presence of MWCNT in the internal structure of the sample. Furthermore, geopolymeric components such as N–A–S–H (sodium aluminosilicate hydrate) or C–A–S–H (calcium aluminosilicate hydrate) appear to contribute to the structure of the sample. Compressive strength tests showed that these components increase the durability of geopolymer concrete. (Table 11)

The chemical composition of the 1% MWCNT + 10% clay reinforced geopolymer concrete sample shows high percentages of Ca (21.53%), Si (15.48%), Na (3.27%), and Al (4.05%). These elements are the primary components

of the sample. Ca and Si are indicative of the presence of geopolymeric components like calcium aluminosilicate hydrate (C–A–S–H) or sodium aluminosilicate hydrate (N–A–S–H), which are fundamental building blocks of geopolymer concrete. These components play a crucial role in enhancing the durability of geopolymer concrete. Literature research indicates that the overall performance of geopolymers improves with the addition of an appropriate amount of calcium component (Yip et al. 2008; Ankur and Siddique 2017). (Table 12)

The chemical composition of the 1.5% MWCNT + 10% Clay reinforced geopolymer sample is very rich and contains various elements in Fig. 18. The percentages of these elements determine the composition of the sample. The elements with particularly high percentages are Si 20.10%, Al 6.80%, Ca 13.17% and Na 5.77%. These elements constitute the main components of the sample. Silicon (Si) is present in a high proportion and indicates the presence of silica or glass-like minerals, one of the main components

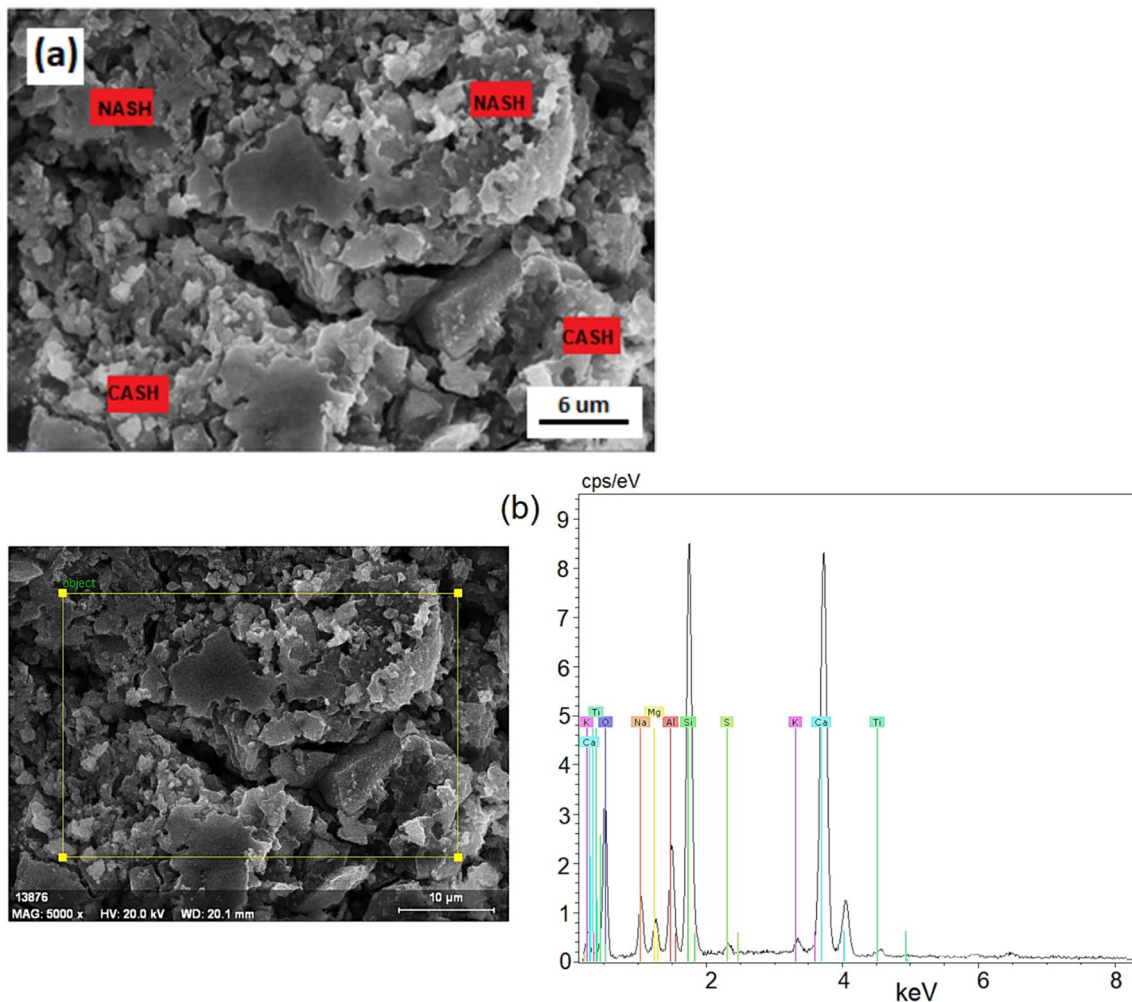


Fig. 17 SEM image **a** and EDS graph of S2-3 (1.0% MWCNT + 10% Clay) geopolymer sample

of the geopolymer matrix. Aluminum (Al) and calcium (Ca) indicate the presence of aluminosilicate minerals and geopolymeric components such as calcium aluminosilicate hydrate (C–A–S–H).

As a result, when the characterization of the geopolymer samples was examined, it was seen that the amount of MWCNT in 0.25% MWCNT + 10% Clay Additive Geopolymer samples had a limited effect on the mechanical properties of the matrix due to the low amount of MWCNT. SEM analysis showed a slight improvement in the structure of the matrix. The mechanical strength of the matrix increased significantly as the amount of MWCNT increased in the 0.5% MWCNT + 10% Clay reinforced Geopolymer samples. SEM analyses showed that MWCNT was well dispersed in the matrix and contributed to the compactness of the matrix.

In 1% MWCNT + 10% Clay reinforced Geopolymer samples, the mechanical strength of the matrix was further increased with 1% MWCNT reinforcement. SEM

analysis confirmed that the dispersion of MWCNT in the matrix increased the hardness and strength of the matrix. Finally, in 1.5% MWCNT + 10% Clay reinforcement Geopolymer samples, 1.5% MWCNT reinforcement significantly increased the flexural and compressive strength of the matrix. SEM analysis showed that MWCNT has a homogeneous distribution in the matrix and strengthened the mechanical properties of the matrix. Studies comparing the mineralogical and structural characteristics of Portland cement and geopolymer concretes, including the formation of CSH (calcium silicate hydrate) and CASH (calcium aluminosilicate hydrate) gels during curing under identical conditions and for equal durations, have revealed significant differences in mineralogical and structural properties. These findings are consistent with previous research in the field (Fernández-Jiménez et al. 2003; Skibsted et al. 1998; Lecomte et al. 2006).

In general, the mechanical properties of MWCNT and clay-reinforced geopolymer samples demonstrated

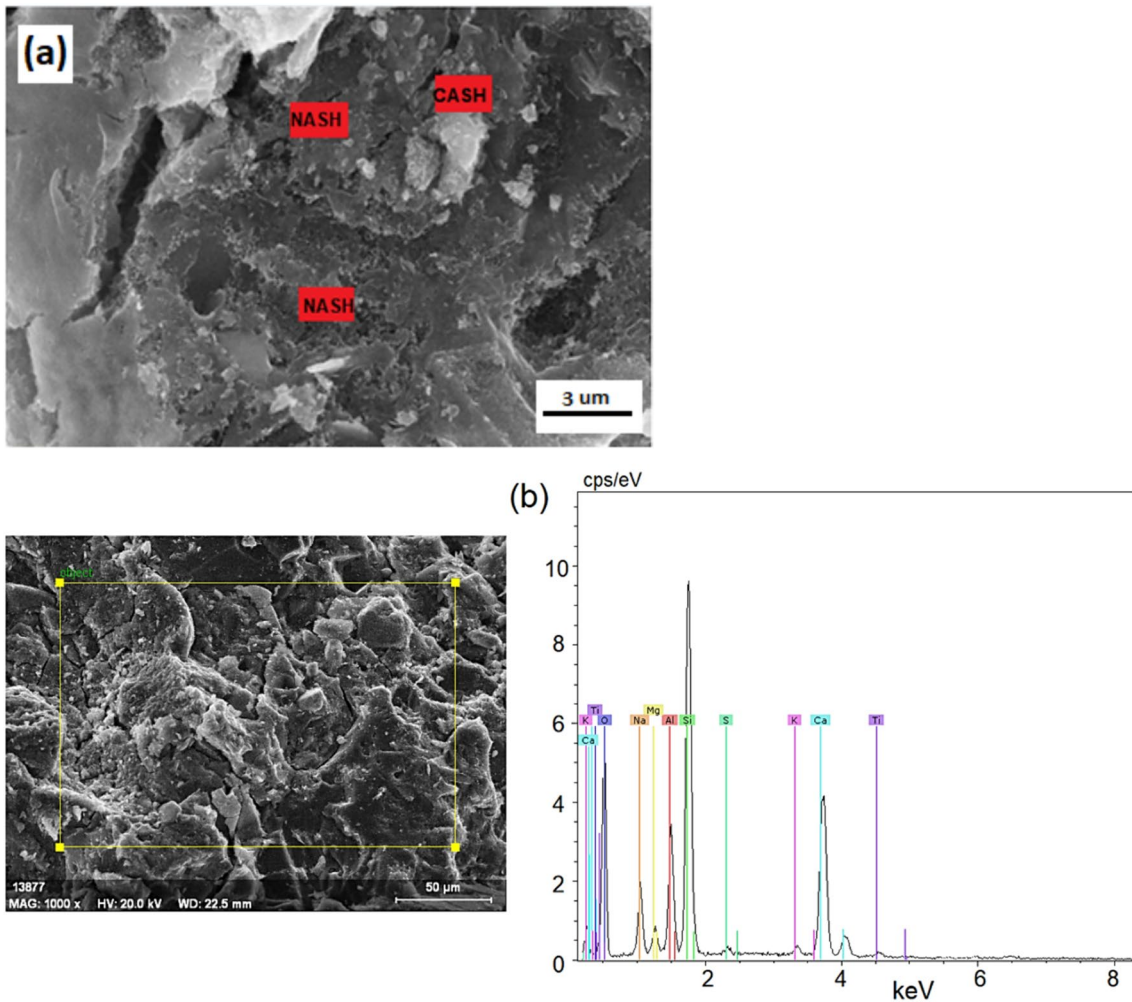


Fig. 18 SEM image a and EDS graph b of S2-4 (1.5% MWCNT + 10% Clay) geopolymer sample

Table 9 S2-1 (0.25% MWCNT + 10% Clay) geopolymer sample EDS analysis

Element	Series	Net	Unn.C (wt.-%)	Norm.C (wt.-%)	Oxid	Oxid.C (wt.-%)
Sodium	K	4356	4.44	4.40	–	–
Magnesium	K	3035	2.17	2.16	Na ₂ O	7.06
Aluminium	K	9229	5.40	5.35	Al ₂ O ₃	12.03
Silicon	K	32,687	17.72	17.57	SiO ₂	44.72
Sulfur	K	894	0.48	0.47	SO ₃	1.41
Potassium	K	1225	0.65	0.64	K ₂ O	0.92
Calcium	K	28,892	16.74	16.60	CaO	27.63
Titanium	K	809	0.69	0.68	TiO ₂	1.35
Manganese	K	577	0.73	0.73	MnO	1.12
Iron	K	482	0.71	0.70	Fe ₂ O ₃	1.20
Oxygen	K	11,391	51.13	50.70	–	–

improvement with increasing MWCNT content. SEM analyses confirmed the homogeneous dispersion of MWCNT

within the matrix. These findings suggest that these materials hold significant potential for developing more durable

Table 10 S2-2 (0.5% MWCNT + 10% Clay) geopolymer sample EDS analysis

Element	Series	Net	Unn.C (wt.-%)	Norm.C (wt.-%)	Oxid	Oxid. C (wt.-%)
Sodium	K	6669	5.67	4.94	–	–
Magnesium	K	2353	1.42	1.24	Na ₂ O	7.94
Aluminium	K	11,220	5.49	4.78	Al ₂ O ₃	10.77
Silicon	K	56,192	25.62	22.30	SiO ₂	56.90
Sulfur	K	905	0.43	0.37	SO ₃	1.11
Potassium	K	898	0.42	0.37	K ₂ O	0.53
Calcium	K	26,476	13.56	11.80	CaO	19.69
Titanium	K	503	0.38	0.33	TiO ₂	0.66
Iron	K	520	0.63	0.55	Fe ₂ O ₃	0.93
Oxygen	K	22,160	61.27	53.33	–	–

Table 11 S2-3 (1.0% MWCNT + 10% Clay) geopolymer sample EDS analysis

Element	Series	Net	Unn.C (wt.-%)	Norm.C (wt.-%)	Oxid	Oxid. C (wt.-%)
Sodium	K	4083	3.27	3.56	–	–
Magnesium	K	2282	1.27	1.38	Na ₂ O	5.64
Aluminium	K	9006	4.05	4.40	Al ₂ O ₃	9.78
Silicon	K	37,496	15.48	16.82	SiO ₂	42.36
Sulfur	K	287	0.12	0.13	SO ₃	0.37
Potassium	K	1788	0.68	0.74	K ₂ O	1.05
Calcium	K	53,008	21.53	23.38	CaO	38.53
Titanium	K	549	0.30	0.32	TiO ₂	0.63
Oxygen	K	11,661	45.37	49.28	–	–

Table 12 S2-4 (1.5% MWCNT + 10% Clay) geopolymer sample EDS analysis

Element	Series	Net	Unn.C (wt.-%)	Norm.C (wt.-%)	Oxid	Oxid. C (wt.-%)
Sodium	K	5585	5.77	5.47	–	–
Magnesium	K	2236	1.66	1.57	Na ₂ O	9.06
Aluminium	K	11,313	6.80	6.44	Al ₂ O ₃	14.97
Silicon	K	35,376	20.10	19.04	SiO ₂	50.12
Sulfur	K	512	0.29	0.28	SO ₃	0.85
Potassium	K	844	0.47	0.45	K ₂ O	0.66
Calcium	K	21,939	13.17	12.48	CaO	21.48
Titanium	K	555	0.47	0.45	TiO ₂	0.92
Oxygen	K	14,987	56.82	53.83	–	–

and sustainable structures in the construction industry and infrastructure projects.

4 Conclusion

In this study, the electrical conductivity properties, mechanical strength effects and workability properties of geopolymer composites containing blast furnace slag, calcined clay and MWCNT were investigated in detail and the results are given below.

- According to the results of mechanical strength tests, it was found that MWCNT reinforcement increased the compressive and flexural strengths of geopolymer composites. In particular, it was observed that samples with 0.25% MWCNT reinforced provided a significant increase in mechanical strength values. This shows that MWCNT has the potential to improve mechanical properties in the matrix.
- The results of the flow diameter tests show that different MWCNT ratios affect the workability properties of geopolymer mortar concrete. It was found that the samples with 0.25% MWCNT content had lower flow

diameter. This indicates that the MWCNT content positively affects the workability up to a certain level, but the reinforcement of higher proportions may adversely affect the workability performance.

- The results show that the addition of MWCNT significantly improves the electrical conductivity properties of geopolymer composites. In particular, the samples with 1% MWCNT reinforcement exhibited high conductivity values. This indicates that these composites can be used in applications requiring electromagnetic conductivity.
- SEM image analysis showed the homogeneous distribution of MWCNTs in the matrix and their interaction with the matrix, and also revealed the effect of clay reinforcement on the matrix structure. It was observed that the mechanical properties of geopolymer samples with different levels of MWCNT and clay reinforcement improved and this improvement became more pronounced with increasing MWCNT content. SEM analyses confirmed that MWCNT has a homogeneous distribution within the matrix and increases the mechanical strength of the matrix.
- XRD results showed that MWCNT and clay reinforcement affect the crystal structure of the matrix. The MWCNT reinforcement led to changes in the crystal structure of the matrix and the clay reinforcement was found to affect the intrinsic structure of the matrix.

As a result, it has shown that geopolymer composites containing blast furnace slag, calcined clay and MWCNT can be evaluated as a potential building material in the construction industry. The high conductivity, mechanical strength and workability properties of these materials are of great importance for the control of structural damage and the development of durable construction materials. Further research and practical testing will provide more information on the performance and behavior of these composites in the future.

Author contributions A.F. conceived the research idea and designed the experimental methodology. R.Y. and M.P. conducted the experiments and collected the data. A.F. and R.Y. analyzed and interpreted the experimental results. A.F. drafted the manuscript, and R.Y. and M.P. provided critical revisions. All authors approved the final version of the manuscript for submission.

Declarations

Conflict of interest All authors confirm that they have no conflicts of interest.

Ethical Approval All authors approve that the research was performed under all the ethical norms.

Consent to publish All authors consent to publish this paper.

Consent to participate Not applicable.

References

- Abu Al-Rub Rashid K, Tyson BM, Yazdanbakhsh A, Grasley Z (2012) Mechanical properties of nanocomposite cement incorporating surface-treated and untreated carbon nanotubes and carbon nanofibers. *J Nanomech Micromech* 2(1):1–6. [https://doi.org/10.1061/\(asce\)nm.2153-5477.0000041](https://doi.org/10.1061/(asce)nm.2153-5477.0000041)
- Akbar FA, Naji M, Dithinde M, Firoozi AA (2021) A review: influence of potential nanomaterials for civil engineering projects. *Iran J Sci Technol - Trans Civ Eng* 45(4):2057–2068. <https://doi.org/10.1007/s40996-020-00474-x>
- Alireza B, Hadianfard MA, Jahangiri M (2024) The influences of type, length, and volumetric fraction of fibers on the direct shear strength of the fiber-reinforced concretes. *Constr Build Mater* 428:136375. <https://doi.org/10.1016/J.CONBUILDMAT.2024.136375>
- Ankur M, Siddique R (2017) Properties of low-calcium fly ash based geopolymer concrete incorporating OPC as partial replacement of fly ash. *Constr Build Mater* 150:792–807. <https://doi.org/10.1016/J.CONBUILDMAT.2017.06.067>
- Babalu R, Pimplikar SS (2022) Influence of nano silica on durability properties of concrete. *Innov Infrastruct Solut* 7(2):1–9. <https://doi.org/10.1007/s41062-022-00777-0>
- Brough AR, Atkinson A (2002) Sodium silicate-based, alkali-activated slag mortars: part I. Strength, hydration and microstructure. *Cem Concr Res* 32(6):865–879. [https://doi.org/10.1016/S0008-8846\(02\)00717-2](https://doi.org/10.1016/S0008-8846(02)00717-2)
- Buchit M, Sukontasukkul P, Sua-Iam G, Sappakittipakorn M, Intarabut D, Suksiripattanapong C, Chindaprasirt P, Limkatanyu S (2021) Mechanical properties and electrical resistivity of multiwall carbon nanotubes incorporated into high calcium fly ash geopolymer. *Case Stud Constr Mater* 15:e00785. <https://doi.org/10.1016/J.CSCM.2021.E00785>
- Burciaga-Díaz O, Durón-Sifuentes M, Díaz-Guillén JA, Escalante-García JI (2020) Effect of waste glass incorporation on the properties of geopolymers formulated with low purity metakaolin. *Cem Concr Compos* 107:103492. <https://doi.org/10.1016/J.CEMCONCOMP.2019.103492>
- Chong Ken P, Garboczi EJ (2002) Smart and designer structural material systems. *Prog Struct Eng Mater* 4(4):417–430. <https://doi.org/10.1002/pse.134>
- Company of the Nanografi Nanotechnology Inc. (2019) 1910 (Category 3)
- Congqi L, Zhou Y, Liu Y, Ren Z, Wang J, Yuan L, Shuang Du, Zhou Z, Huang Y (2022) Effects of nano-SiO₂, nano-CaCO₃ and nano-TiO₂ on properties and microstructure of the high content calcium silicate phase cement (HCSC). *Constr Build Mater* 314:125377. <https://doi.org/10.1016/J.CONBUILDMAT.2021.125377>
- Dieu NQ, Castel A (2023) Developing geopolymer concrete by using ferronickel slag and ground-granulated blast-furnace slag. *Ceramics* 6(3):1861–1878. <https://doi.org/10.3390/ceramics6030114>
- Drabczyk A, Kudłacik-Kramarczyk S, Korniejenko K, Figiela B, Furtos G (2023) Review of geopolymer nanocomposites: novel materials for sustainable development. *Materials* 16(9):3478. <https://doi.org/10.3390/ma16093478>
- Enrique G-M, D'Alessandro A, Castro-Triguero R, Pérez-Mira D, Ubertini F (2017) Micromechanics modeling of the electrical conductivity of carbon nanotube cement-matrix composites. *Compos Part B Eng* 108:451–469. <https://doi.org/10.1016/J.COMPOSITESB.2016.10.025>

- Eun OJ, Monteiro PJM, Jun SS, Choi S, Clark SM (2010) The evolution of strength and crystalline phases for alkali-activated ground blast furnace slag and fly ash-based geopolymers. *Cem Concr Res* 40(2):189–196. <https://doi.org/10.1016/J.CEMCONRES.2009.10.010>
- Fangming Du, Scogna RC, Zhou W, Brand S, Fischer JE, Winey KI (2004) Nanotube networks in polymer nanocomposites: rheology and electrical conductivity. *Macromolecules* 37(24):9048–9055. <https://doi.org/10.1021/ma049164g>
- Fernández-Jiménez A, Puertas F, Sobrados I, Sanz J (2003) Structure of calcium silicate hydrates formed in alkaline-activated slag: influence of the type of alkaline activator. *J Am Ceram Soc* 86(8):1389–1394. <https://doi.org/10.1111/j.1151-2916.2003.tb03481.x>
- Gowda Raje H, Narendra DR, Prabhakar R (2017) Effect of nano-alumina on workability, compressive strength and residual strength at elevated temperature of cement mortar. *Mater Today Proc* 4(11):12152–12156. <https://doi.org/10.1016/J.MATPR.2017.09.144>
- Hawreen A, Bogas JA, Kurda R (2019) Mechanical characterization of concrete reinforced with different types of carbon nanotubes. *Arab J Sci Eng* 44(10):8361–8376. <https://doi.org/10.1007/s13369-019-04096-y>
- Heydar D, Yilmaz K (2021) A more sustainable approach for producing less expensive electrically conductive concrete mixtures: experimental and Fe study. *Cold Reg Sci Technol* 184:103231. <https://doi.org/10.1016/J.COLDREGIONS.2021.103231>
- Hieu DN, Van Tran H, Choi KK (2020) Direct shear behavior of cementitious mortar reinforced by carbon fiber textile. *Constr Build Mater* 249:118760. <https://doi.org/10.1016/J.CONBUILD-MAT.2020.118760>
- Ismael Mustafa K (2022) Mechanical properties of nanotubes. Graphene, nanotub quantum dots-based nanotechnol fundam appl January 445–80 <https://doi.org/10.1016/B978-0-323-85457-3.00005-0>
- Jang Daeik HN, Yoon SZ, Farooq HK, Lee, and I. W. Nam, (2021) Influence of water ingress on the electrical properties and electromechanical sensing capabilities of CNT/cement composites. *J Build Eng* 42:103065. <https://doi.org/10.1016/j.jobe.2021.103065>
- Jang Daeik HN, Yoon JS, Yang B, Jang JG, Park S (2023) Effect of carbonation curing regime on electric heating performance of CNT/cement composites. *J Build Eng* 73:106815. <https://doi.org/10.1016/j.jobe.2023.106815>
- Kamal K, Pandey A, Wagri NK, Saxena A, Patel J, Al-Fakih A (2023) Technological challenges in nanoparticle-modified geopolymer concrete: a comprehensive review on nanomaterial dispersion, characterization techniques and its mechanical properties. *Case Stud Constr Mater* 19:e02265. <https://doi.org/10.1016/J.CSCM.2023.E02265>
- Khalid SM, Shobha MS (2023) Effect of ternary blends on mechanical strength, durability and microstructural properties of geopolymer concrete. *Iran J Sci Technol, Trans Civil Eng* 16:1–7. <https://doi.org/10.1007/s40996-023-01241-4>
- Khater HM, Abd El Gawaad HA (2016) Characterization of alkali activated geopolymer mortar doped with MWCNT. *Constr Build Mater* 102:329–337. <https://doi.org/10.1016/J.CONBUILDMAT.2015.10.121>
- Khater HM, El-Nagar AM (2020) Preparation of sustainable of eco-friendly mwcnt-geopolymer composites with superior sulfate resistance. *Adv Compos Hybrid Mater* 3(3):375–389. <https://doi.org/10.1007/s42114-020-00170-4>
- Kim HK, Nam IW, Lee HK (2014a) Enhanced effect of carbon nanotube on mechanical and electrical properties of cement composites by incorporation of silica fume. *Compos Struct* 107:60–69. <https://doi.org/10.1016/J.COMPSTRUCT.2013.07.042>
- Kim HK, Park IS, Lee HK (2014b) Improved piezoresistive sensitivity and stability of CNT/cement mortar composites with low water-binder ratio. *Compos Struct* 116(1):713–719. <https://doi.org/10.1016/j.compstruct.2014.06.007>
- Kim GM, Yang BJ, Cho KJ, Kim EM, Lee HK (2017) Influences of CNT dispersion and pore characteristics on the electrical performance of cementitious composites. *Compos Struct* 164:32–42. <https://doi.org/10.1016/j.compstruct.2016.12.049>
- Kordkheili HY, Shehni SE, Niyatzade G (2015) Effect of carbon nanotube on physical and mechanical properties of natural fiber/glass fiber/cement composites. *J for Res* 26:247–251. <https://doi.org/10.1007/s11676-014-0003-y>
- Lecomte I, Henrist C, Liégeois M, Maseri F, Rulmont A, Cloots R (2006) (Micro)-Structural comparison between geopolymers, alkali-activated slag cement and portland cement. *J Eur Ceram Soc* 26(16):3789–3797. <https://doi.org/10.1016/J.JEURCERAMSOC.2005.12.021>
- Leone M, Centonze G, Colonna D, Micelli F, Aiello MA (2018) Fiber-reinforced concrete with low content of recycled steel fiber: shear behaviour. *Constr Build Mater* 161:141–155. <https://doi.org/10.1016/J.CONBUILDMAT.2017.11.101>
- MacKenzie Kenneth JD, Bolton MJ (2009) Electrical and mechanical properties of aluminosilicate inorganic polymer composites with carbon nanotubes. *J Mater Sci* 44(11):2851–2857. <https://doi.org/10.1007/s10853-009-3377-z>
- Meng Li, Xing D, Zheng QB, Li H, Hao B, Ma PC (2022) Variation on the morphology and tensile strength of basalt fiber processed in alkali solutions. *Constr Build Mater* 335:127512. <https://doi.org/10.1016/j.conbuildmat.2022.127512>
- Mesgari AS, Ahmadi H, Khalaj G, Ghasemi B (2016) Microstructure and mechanical properties of a metakaolinite-based geopolymer nanocomposite reinforced with carbon nanotubes. *Ceram Int* 42(14):15171–15176. <https://doi.org/10.1016/J.CERAMINT.2016.06.080>
- Mohamed S, Andrew K, Tang PL, McGhon D, Taylor S, Rahman M, Yang S, Zhou X (2013) Multifunctional properties of carbon nanotube/fly ash geopolymeric nanocomposites. *Constr Build Mater* 49:46–55. <https://doi.org/10.1016/J.CONBUILDMAT.2013.08.007>
- Moraes JCB, Akasaki JL, Melges JLP, Monzó J, Borrachero MV, Soriano L, Payá J, Tashima MM (2015) Assessment of sugar cane straw ash (SCSA) as pozzolanic material in blended portland cement: microstructural characterization of pastes and mechanical strength of mortars. *Constr Build Mater* 94:670–677. <https://doi.org/10.1016/J.CONBUILDMAT.2015.07.108>
- Morsy MS, Alsayed SH, Aqel M (2011) Hybrid effect of carbon nanotube and nano-clay on physico-mechanical properties of cement mortar. *Constr Build Mater* 25(1):145–149. <https://doi.org/10.1016/j.conbuildmat.2010.06.046>
- Nawaz M, Heitor A, Sivakumar M (2020) Geopolymers in construction-recent developments. *Constr Build Mater* 260:120472. <https://doi.org/10.1016/J.CONBUILDMAT.2020.120472>
- Nguyen TN, Yoo DY, Kim JJ (2020) Cementitious material reinforced by carbon nanotube-nylon 66 hybrid nanofibers: mechanical strength and microstructure analysis. *Mater Today Commun* 23:100845. <https://doi.org/10.1016/j.mtcomm.2019.100845>
- Panjasil P, Pinitsoonthorn S, Thongbai P, Amornkitbamrung V, Chindaprasit P (2018) Effects of carbon fiber on mechanical and electrical properties of fly ash geopolymer composite. *Mater Today Proc* 5(6):14017–14025. <https://doi.org/10.1016/J.MATPR.2018.02.054>
- Pekmezci B, Arabacı E (2021) Binalarda kullanılan yapısal olmayan kompozit panellerin fiziksel ve mekanik özelliklerinin değerlendirilmesi. *Gazi Üniversitesi Mühendislik Mimarlık Fakültesi Dergisi* 36(3):1347–1360. <https://doi.org/10.17341/gazimmfd.769811>

- Puertas F, Palacios M, Manzano H, Dolado JS, Rico A, Rodríguez J (2011) A model for the C–A–S–H gel formed in alkali-activated slag cements. *J Eur Ceram Soc* 31(12):2043–2056. <https://doi.org/10.1016/J.JEURCERAMSOC.2011.04.036>
- Sawarkar PG, Pote A, Murmu AL (2023) Properties of blast furnace slag geopolymer concrete. *Mater Today Proc*. <https://doi.org/10.1016/J.MATPR.2023.03.179>
- Skibsted J, Jakobsen HJ, Hall Ch (1998) Quantitative aspects of 27Al MAS NMR of calcium aluminoferrites. *Adv Cem Based Mater* 7(2):57–59. [https://doi.org/10.1016/S1065-7355\(97\)00017-5](https://doi.org/10.1016/S1065-7355(97)00017-5)
- Torres-Carrasco M, Puertas F (2015) Waste glass in the geopolymer preparation. mechanical and microstructural characterisation. *J Clean Prod* 90:397–408. <https://doi.org/10.1016/J.JCLEPRO.2014.11.074>
- Vivek D, Elango KS, Saravanakumar R, Rafek BM, Ragavendra P, Kaviarasan S, Raguram E (2021) Effect of nano-silica in high performance concrete. *Mater Today: Proc* 37:1226–1229. <https://doi.org/10.1016/J.MATPR.2020.06.431>
- Xingyi Z, Gao Y, Dai Z, Corr DJ, Shah SP (2018) Effect of interfacial transition zone on the Young's modulus of carbon nanofiber reinforced cement concrete. *Cem Concr Res* 107:49–63. <https://doi.org/10.1016/J.CEMCONRES.2018.02.014>
- Yip CK, Lukey GC, Provis JL, van Deventer JSJ (2008) Effect of calcium silicate sources on geopolymerisation. *Cem Concr Res* 38(4):554–564. <https://doi.org/10.1016/J.CEMCONRES.2007.11.001>
- Yoon HN, Jang D, Kil T, Lee HK (2023) Influence of various deterioration factors on the electrical properties of conductive cement paste. *Constr Build Mater* 367:130289. <https://doi.org/10.1016/j.conbuildmat.2022.130289>
- Younesi KH, Hiziroglu S, Farsi M (2012) Some of the physical and mechanical properties of cement composites manufactured from carbon nanotubes and bagasse fiber. *Mater Des* 33(1):395–398. <https://doi.org/10.1016/J.MATDES.2011.04.027>
- Yu R, Spiesz P, Brouwers HJH (2014) Static properties and impact resistance of a green ultra-high performance hybrid fibre reinforced concrete (UHPPHRC): experiments and modeling. *Constr Build Mater* 68:158–171. <https://doi.org/10.1016/J.CONBUILD-MAT.2014.06.033>
- Yurdakul A (2022) Elevated temperature effects on fly ash-based geopolymer composites produced with waste granite Dust. *Iran J Sci Technol Trans Civ Eng* 46(6):4205–4217. <https://doi.org/10.1007/s40996-022-00862-5>
- Zhidan R, Sun W, Xiao H, Jiang G (2015) Effects of nano-SiO₂ particles on the mechanical and microstructural properties of ultra-high performance cementitious composites. *Cem Concr Compos* 56:25–31. <https://doi.org/10.1016/J.CEMCONCOMP.2014.11.001>
- Zijian Su, Hou W, Sun Z (2020) Recent Advances in Carbon Nanotube-Geopolymer Composite. *Constr Build Mater* 252:118940. <https://doi.org/10.1016/J.CONBUILDMAT.2020.118940>

Springer Nature or its licensor (e.g. a society or other partner) holds exclusive rights to this article under a publishing agreement with the author(s) or other rightsholder(s); author self-archiving of the accepted manuscript version of this article is solely governed by the terms of such publishing agreement and applicable law.